

MPPT Solar Battery Charger

ECE 499: Design Project II

August 6th 2024



University
of Victoria



Group ID: 12

Faculty supervisor: Michael McGuire

Team Information:

S. No.	Name	V Number
1	Nikhil Sharma	V01025628
2	Lawrence Chan	V01025675
3	Logan Winter	V01026189
4	Mclaine De Jesus	V00882180
5	Brett Dionello	V01026046



Acknowledgment

We would like to extend our sincere gratitude to all those who contributed to the successful completion of this project.

Firstly, our heartfelt thanks go to our Project Supervisor and the Chairman of the Electrical & Computer Engineering department, Dr. Michael McGuire, whose guidance and support were invaluable throughout the project and his generous funding and financial support, which made this project possible.

Our appreciation extends to our Teaching Assistant, Mr. Brian Zhu, for his insightful feedback and support throughout this project ensuring we met all our deadlines and milestones.

Next, we would like to acknowledge and respect the Lək'ʷəŋən (Songhees and Esquimalt) Peoples on whose territory the university stands, and the Lək'ʷəŋən and WSÁNEĆ Peoples whose historical relationships with the land continue to this day.

Finally, we would like to express our deep gratitude to our family and friends for their unwavering encouragement and support during this endeavor.

Thank you all for your contributions and support.

Contents

Executive Summary	1
I Introduction	2
II Objectives.....	3
III Literature Survey	3
Existing Technology and Market.....	3
DC-DC Conversion.....	4
Maximum Power Point Tracking (MPPT) Algorithms.....	6
Battery Choice Review:.....	7
IV Team Duties & Project Planning	9
V Design Methodology, Analysis, and Specifications	10
Design methodology	10
Specifications	15
VI Design Prototype, and Testing.....	16
Design Prototype.....	16
Software Design.....	16
Hardware Design.....	20
VII Prototype Testing	23
Test setup.....	23
Initial Startup test	25
Full-sunlight test.....	25
Efficiency Test	26
Discarded tests.....	26
VIII Cost Analysis	26
Direct Costs.....	26
Indirect Costs.....	27
Funding.....	27
Tentative Pricing and Return on Investment (ROI)	28
Cost Reduction Strategies	28
IX Conclusion & Recommendations	28
References.....	29
Appendix.....	30
Code of ethics of EGBC.....	30
Website link and the main page image.....	31
Details of data, test results	31
Overall Test Plan.....	33

Executive Summary

Our project addresses the challenge of solar power inefficiency by developing a cost-effective, open-source Maximum Power Point Tracker (MPPT) system. Traditional Pulse Width Modulation (PWM) charge controllers often fall short in matching solar panel outputs with battery storage needs, limiting their effectiveness. Our solution aims to optimize energy capture and storage through a sophisticated MPPT algorithm.

We employed the SPRINT design methodology, which encompasses six key phases. First, we defined the problem: solar panels typically operate at only 15-20% efficiency. Our goal was to create a flexible, easily modifiable MPPT system that improves energy capture. In the literature review phase, we explored existing solutions and alternative designs. Based on feedback, we decided against an RTOS-based system and used simulations with MATLAB and SIMULINK to guide our component choices. We selected a SEPIC converter for its broad voltage range and lower noise, over traditional buck-boost and flyback topologies.

During the simulation and testing phase, we examined the impact of partial shading, which couldn't be fully replicated in simulations but will be addressed in practical tests. We focused on the Incremental Conductance MPPT algorithm and opted for continuous mode to avoid transient issues. An irradiance sweep analysis helped us understand how varying irradiance affects panel output and PWM duty cycles, which informed our design specifications.

Our specifications, based on a 100W solar panel, include an input voltage range of 5V to 50V, an output voltage of 15V, an output current of 8A, a PWM frequency of 50kHz, and a temperature range of 15°C to 100°C. Component values were calculated for inductors, capacitors, and duty cycles to ensure durability and performance, with components scaled up to handle potential transients.

In conclusion, our MPPT system addresses solar power inefficiencies by enhancing energy capture and storage, supporting continuous device operation, and promoting sustainable energy practices. This system aligns with the Engineers and Geoscientists BC (EGBC) Code of Ethics by advancing environmental stewardship and reducing fossil fuel reliance. The project exemplifies a commitment to green energy solutions, aiming to foster a more sustainable and eco-friendly future. Future work could focus on optimizing battery charge algorithms, exploring advanced MPPT algorithms, integrating Internet of Things (IoT) technology for efficiency tracking, and improving DC-DC converters to reduce energy losses.

I Introduction

One major issue with solar power is that its efficiency varies with the current drawn from the panel, leading to less power being captured when the voltage or current is not ideal. Traditional PWM charge controllers, which are used to store energy in batteries, require a close match between the panel's output and the battery, limiting flexibility and effectiveness. Our small-scale, low-cost, open-source solution addresses these issues by using a Maximum Power Point Tracker (MPPT) algorithm. This approach adjusts to the varying conditions of the solar panel to ensure the maximum possible energy is captured and stored, making solar power more efficient and adaptable.

Implementing a MPPT system with a buck-boost converter allows a greater range of input voltages, thus allowing more variety in solar panel configurations. Furthermore, we can minimize losses in the system and expand the window of usable irradiance. The solar panel will supply power to a device while simultaneously charging a battery which will supply the load should the solar panel fail to deliver sufficient power. This way the device in question is operational for the maximum duration (dependant on the battery used), while sustaining battery performance as long as possible. To do this our team aims to design and implement a robust Maximum Power Point Tracker (MPPT) system optimized for efficient utilization of solar energy. Specifically, our aim is to develop a self-sustaining MPPT solution capable of maximizing the power output derived from solar panels over varying environmental conditions. This system will be engineered to power devices such as heaters, ensuring reliable and continuous energy supply without reliance on traditional power grids or fossil fuels. Our group selected this project with a commitment to advancing green energy solutions and enhancing power efficiency through renewable sources. By harnessing the full potential of solar energy, we aim to contribute to sustainable practices and reduce the carbon footprint associated with conventional energy consumption. This project not only aligns with our passion for environmental stewardship but also provides practical benefits to diverse user groups.

Our project upholds Principle 1 of the Engineers and Geoscientists BC (EGBC) Code of Ethics by optimizing solar energy efficiency, thereby promoting sustainable development and environmental stewardship. The MPPT system maximizes renewable energy generation and reduces reliance on fossil fuels, contributing to mitigating climate change impacts and enhancing overall energy sustainability. We also adhere to Principle 2 as our team consists of electrical engineers trained in hardware and software development, ensuring competence in our project focus. Compliance with Principle 11 is demonstrated by listing all team members and their contributions transparently. Additionally, Principle 13 guides us to conduct our work in good faith, acknowledging and crediting the relevant sources we have referenced throughout our project.

Individuals looking to maximize power collection from alternative energy where resources are limited will find our MPPT system invaluable, as it offers a portable and reliable power source for small to potentially large devices, solely powered by solar panels. This capability enhances convenience and sustainability in remote or off-grid locations, where access to conventional power sources may be limited. Moreover, owners of residential, commercial, or industrial solar energy systems stand to benefit

significantly from our MPPT technology. By optimizing energy efficiency and output, our system supports a higher return on investment for solar installations, making renewable energy solutions more economically attractive and environmentally beneficial. This, in turn, encourages broader adoption of solar panels among businesses and homeowners, thereby reducing dependence on fossil fuels and promoting a greener future. Additionally, regulatory bodies and organizations promoting renewable energy adoption, such as government agencies in the renewable energy sector, will find our MPPT system valuable for assessing and verifying the performance of solar panel installations. By ensuring compliance with energy efficiency standards and environmental regulations, our technology contributes to the growth and sustainability of renewable energy initiatives at a national and global scale.

II Objectives

- (i) To design and implement a Maximum Power Point Tracking (MPPT) system that efficiently manages both the charging of a battery and the supply of power to a load from a solar panel.
- (ii) To integrate real-time power measurement and monitoring features to accurately track and optimize the energy delivered by the solar panel.
- (iii) To develop a self-sustaining solar power system that operates autonomously over extended periods without requiring external power sources.
- (iv) To analyze existing MPPT solutions and design options, selecting the most effective algorithms and hardware to optimize solar energy capture and battery charging.
- (v) To perform detailed simulations of the MPPT system to validate and refine the design, ensuring it meets performance and efficiency criteria before building the physical prototype.
- (vi) To build and test a functional prototype of the MPPT system, demonstrating its capabilities and performance through a comprehensive presentation, and showcasing its practical benefits in real-world applications.

III Literature Survey

Existing Technology and Market

There are many commercially available MPPT systems on the market that offer drop-in solutions for solar power battery charge controllers. The form factor typically is a 6-terminal device with two connectors for each of the positive and negative wires of the solar, battery and load, respectively. The devices come in many sizes/power ratings for different systems ranging from recreational vehicle use to home solar systems and even industrial scale and have price ranges of \$70 to \$600 USD. [1] A charger will have to be designed specifically for a battery type. Some common battery technologies are discussed in the battery review section, where the charging characteristics of the lead-acid battery

are explained. Most available products will be designed for use with lead-acid batteries and will be hard coded to implement the 3-stage charging scheme.

Our product and market position:

The goal of our design is to be used for small scale and very small-scale applications in the 300W range and to be available as a low-cost open-source educational and research platform. The design will allow for some variation input and output voltage ranges to accommodate some different solar panel, battery, and load options. The open-source design will be simple enough to be modified if a larger capacity is required. The ability to implement custom MPPT algorithms and battery management will allow for additional battery chemistry types and testing of different battery charging schemes to maximize system efficiency. It has been shown that further research is still needed to develop efficient charging schemes for valve-regulated lead acid batteries in solar systems. [2] It was reported in a 2018 study that a MPPT system used for a home solar system in Africa would need to cost about \$20USD to be competitive with a direct to battery method. [1] Therefore, it is clear that commercially available products are not yet affordable enough nor are they maximally efficient at charging the most common battery types.

DC-DC Conversion

Due to increasing need for renewable energy generation, there currently is a wide variety of MPPT and PWM battery charge controller solutions available on the market. For smaller applications such PWM controllers see more widespread use due to the lower cost. When compared to MPPT technology PWM controllers use fewer components and are simpler to implement. However, these systems have several setbacks such as the necessity for the solar panel voltage to be above the battery voltage to charge. Depending on the irradiance conditions to the panel, the PV voltage could easily become less than that of the battery while still having the capability to provide power albeit at a lower voltage.

The goal of a PWM switching converter in a solar charge controller is to reduce the voltage, and subsequently the current, to a safe range as required by the battery. However, when reducing the voltage with PWM, the available charging current does not increase and is instead dissipated as a loss of power. More advanced switching converters can be used to recoup those losses and obtain a much greater efficiency, often over 90%. Switching converters can come in isolated and non-isolated switching modes. Three of the most common modes of non-isolated switching converters that are seen in MPPT are buck, boost, and buck-boost. The three circuits can be seen as step-down, step-up, and a combination of step-down and step-up, respectively. Due to the higher component count and need for inductors, these types of converters will incur a greater cost to the final product.

A DC-Chopper circuit, such as that used in a PWM charge controller, steps down the DC output voltage by adjusting the on/off duty cycle of the input voltage. This operation is most likely performed by a buck converter, which works to reduce the input DC voltage while smoothing out the high frequency ripple mostly caused by second and third order harmonics. The output voltage can be calculated as:

$$V_{out} = D \times V_{in}$$

[3]

Where D is the duty cycle of the switch given as a percentage.

A boost converter is a type of DC-DC power converter that steps up the input voltage to a higher output voltage. It operates by periodically storing energy in an inductor during the "on" phase of a switching transistor and then releasing this energy to the output capacitor and load during the "off" phase. When the switch is closed, current flows through the inductor, creating a magnetic field and storing energy. When the switch opens, the inductor's magnetic field collapses, generating a voltage that combines with the input voltage to produce a higher output voltage. [3] The boost converter's output voltage is regulated by adjusting the duty cycle of the switch. In a charge controller, albeit not used as often, the boost converter can bring a source voltage up to a higher potential than the battery so that can be used to charge the battery. The output voltage can be calculated as:

$$V_{out} = V_{in} \times (1 + D)$$

Where D is the duty cycle of the switch given as a percentage.

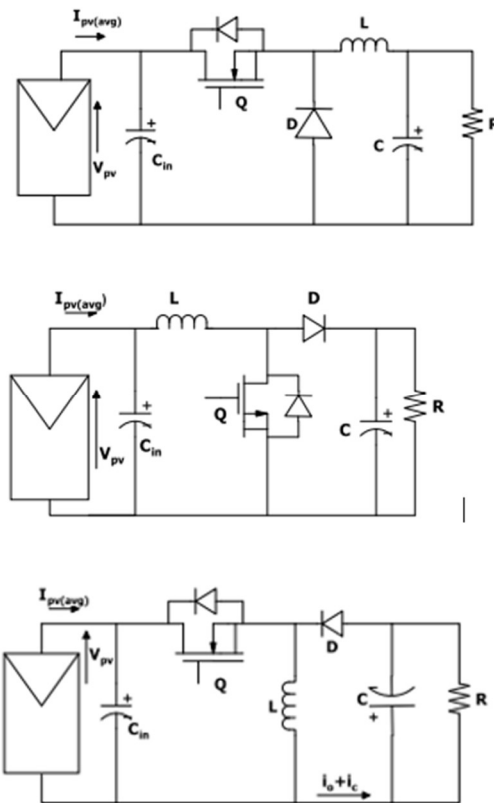


Fig 1: Basic asynchronous topologies of non-isolated switching mode boost topologies; buck circuit (top), boost circuit (middle), buck-boost circuit (bottom). [3]

With respect to MPPT, both the buck and boost circuits can limit the capabilities of obtaining the true maximum power point of the solar array should certain conditions be met. In the case of the buck converter, having a battery configuration with a voltage higher than the ideal maximum power point voltage, V_{mp} , will result in the MPPT algorithm failing to successfully obtain its target. Likewise, for boost converters an MPPT control algorithm will be unable to reduce the solar array voltage to meet V_{mp} . Combining the capabilities of both the buck and boost, the buck-boost converter can provide the MPPT control algorithm the ability to step up or down the voltage if the system sees maximum power points on either side of the battery voltage and is therefore the option we have selected for this project. [4] [5]

Maximum Power Point Tracking (MPPT) Algorithms

When looking into MPPT algorithms there are many different options to choose from, each with pros and cons as well as varying levels of difficulty in implementation. Some of the methods used are explained in the following descriptions:

- Perturb and Observe (P&O) - This method relies on the use of a voltage and current sensor to determine the power output of the PV cells. When the voltage of the PV system is perturbed, the output power either increases or decreases. Comparing the current power output to the previous reading, the algorithm will then continue to perturb the voltage in the same direction if the power has increased, or in the other direction if the power has decreased. [6] The P&O algorithm is relatively simple to implement and moderately efficient but suffers from being slow to track constantly changing weather conditions.

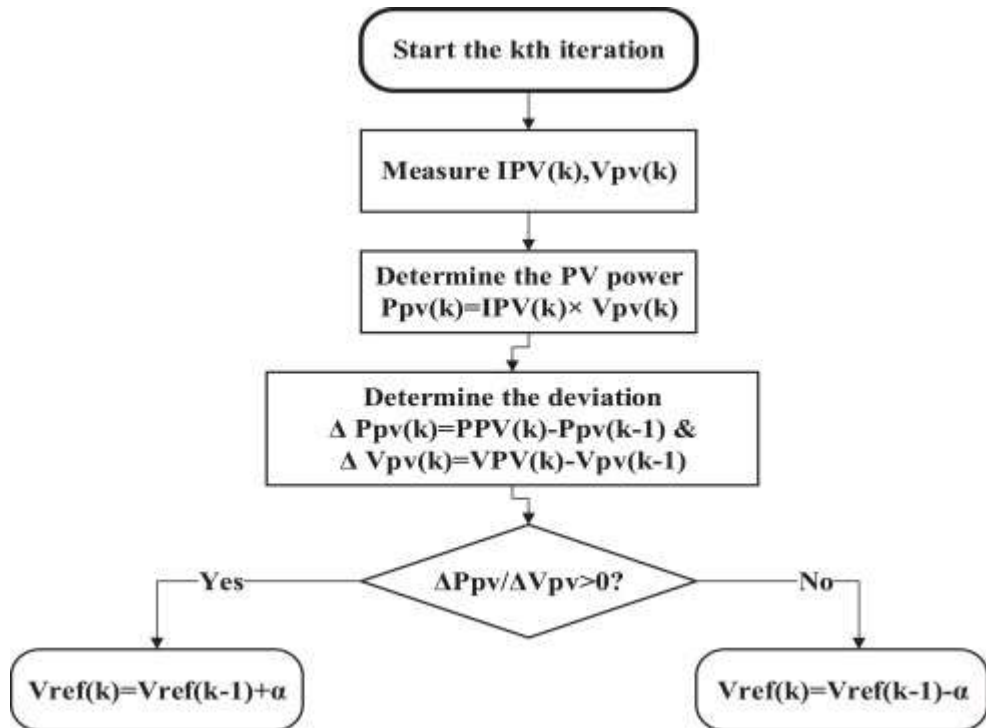


Fig 2: Example of P&O algorithm [6]

- Incremental Conductance - Similarly to perturb and observe, incremental conductance uses both a voltage and current sensor to track the changes over time. Instead of calculating the corresponding power, this algorithm follows the relationship between current and voltage of the PV array as shown in equation 2 [6]. Using this relationship, it can be determined whether the MPP has been met and the direction of the adjustment necessary if it has not been met. The Incremental Conductance algorithm is more complicated to implement than the P&O algorithm but has the advantage of being faster at tracking changes in weather as well as being more efficient as it does not try to make any control actions if MPP has been met.

$$\Delta I_{PV} \Delta V_{PV} = -I_{PV} V_{PV} = 0 \text{ at MPP}$$

- Fuzzy Logic – The basic Fuzzy Logic algorithm uses a fuzzy logic controller which inputs a current value into a fuzzification module to turn it into a function based on the fuzzy set. This fuzzy value is then observed by an inference engine which generates control actions based on a pre-existing rule table. After these control actions have been determined, they are fed into a defuzzification module which converts it from the fuzzy set back to a regular control action. Fuzzy logic is hard to evaluate as the performance varies wildly on the implementation. [6]. While it has the potential to be robust and easy to design, the complexity of the controllers outweighs the pros.

Algorithm Selection:

Based on the pros and cons of the algorithms, incremental conductance is a good compromise between complexity, efficiency and tracking speed.

Battery Choice Review:

For solar system energy storage there are 3 main options used commonly, Lead-Acid (Flooded), Lead-Acid (Sealed) and Lithium-ion. The following is a summary of these battery types which were used to select the battery choice for this project.

Lead-Acid (Flooded) – Consist of two plates of lead (electrodes) which are suspended in a sulfuric acid solution. In the charged state, the battery's chemical energy is stored between metallic lead on the negative side and lead oxide on the positive side. When discharged the lead and dilute acid produce lead sulfate and water. Charging current must be matched to the batteries ability to absorb the energy, too high a current will cause electrolysis which decomposes the water into hydrogen and oxygen (off gassing). [8]

- High surge currents
- Low energy Density
- Cheap
- Suffers from acid stratification (corrected by over-charging)
 - This is the precipitation of acid out of the water, which collects at the bottom of the container and does not contribute to the chemical reaction, since less ions are available for energy transfer.
- Lowest lifespan (500 Cycles) without maintenance
- Needs to be refilled with distilled water due to off gassing

- Long charge times

Sealed-Lead acid (Valve Regulated) – Same chemistry as flooded, but the electrolyte is immobilized. Characterized by a limited amount of electrolyte absorbed in a separator (gel or AGM). Leaves enough space in the enclosure for gases to build up which can then be recombined within the cell, the valve is provided for overpressure situations. The recombination of gases prevents the need for refilling with distilled water. [9]

Benefits over flooded design:

Topping up with water is not necessary (maintenance free), no risk of acid spilling, reduced hydrogen off gassing, lower rate of self-discharging, shorter recharge time, more tolerant to deep cycling.

Two types:

- Gel
 - Best lifespan for lead-acid batteries
 - Highest price for lead-acid batteries
- Absorptive glass mat (AGM)
 - Better price than Gel but more expensive than flooded
 - Cannot use tall cells
 - 500 - 1300 cycles

Lithium-Ion (Li-ion) – Uses the reversible intercalation (insertion of ions into layered materials) of lithium ions into electrically conduction solids that store energy. There are at least 12 types of Li-ion batteries consisting of different chemical compositions for different specialized purposes. Due to the buildup of lithium metal on the anode, careful charging must be implemented to prevent an internal short circuit of the battery and fire/explosion risk. [1]

- Highest initial price
- Difficult charging characteristics
 - Risk of fire/explosion – Thermal runaway
- High energy density and efficiency
- High discharge and recharge rates
- Longer cycle life and calendar than lead-acid (more charge cycles)
 - Reduced replacement costs
- Decreasing price in future

Selected battery type: AGM Lead-acid battery

following the above summary the AGM lead-acid battery was selected as the optimal battery for this project due to the balance between cost and performance as well as minimal maintenance requirements. The Lithium-Ion battery was excluded due to the increased risk of hazard in the context of a school demonstration.

Lead-Acid Battery Charging:

The charging requirements of the lead-acid battery are one of its underlying disadvantages as it has a long recharge cycle that requires three-stages: Bulk charge, absorption charge, and float charge. If these stages are not correctly followed the longevity and capacity of the battery will be reduced. Additionally, for maximum life the battery should be fully charged as soon as possible after a discharge to prevent sulfation (the formation of sulfur trioxide) and kept at a full charge when not in use. A standard

lead-acid should not be discharged to a depth of discharge greater than 50% unless it is specifically a deep-cycle battery which can go to 80% DOD in extreme cases. [10]

Bulk Charge – Fast charging (high current) up to ~70% of capacity. Typically, at a fixed voltage for a few hours.

The current required is defined by the batteries C-rate for the bulk stage

The C-rate is a measure of the rate at which a battery is charged or discharged relative to its capacity.

Absorption stage – Current-tapering off stage

The charge acceptance rate gradually reduces

This stage allows all cells of the battery to equalize to the same voltage

Continue until a voltage setpoint is reached

Float stage – voltage setpoint at an extremely low C-rate

Maintains the battery at a fully charged state indefinitely

Offsets the normal self-discharge rate of the battery

IV Team Duties & Project Planning

The first major hurdle is the hardware design. This was be overseen primarily by Lawrence Chan, and Logan Winter. The hardware team was responsible for the design and testing of the hardware. Lawrence Chan will be designing the power distribution unit (PDU). The PDU will filter, regulate, and route power throughout the device. Additionally, Logan Winter designed a buck-boost converter that was be suitable for our MPPT applications. The final task of the hardware team was the selection and hardware implementation of the STM32 microcontroller. The hardware team is the priority as without the general hardware designs specific software implementation cannot be tested.

Next the software team which consists of Nikhil Sharma, Mclaine De Jesus, and Brett Dionello. Programming the microcontroller and liquid ink display (native teh the STM32 board being used) to display voltage and current values being provided from the solar panel and the battery was be done by Mclaine De Jesus. The microcontroller monitors for overvoltage or other errors in the system while simultaneously managing any calculations that was needed to be done for the MPPT algorithm. Mclaine De Jesus oversaw the selection of the incremental conductance MPPT algorithm that was implemented in software. Brett Dionello worked on creating the UML state diagram as well as implementing the various state conditions depending on the cycle of battery charging. Brett also worked with Nikhil Sharma to create and monitor a PWM signal (controlled by power from the solar panel) that was used to control the boost-buck converter.

There were some roadblocks that came up during the design process which in turn threw off the timing of work. For example, the prototype hardware was experiencing lots of ringing on the input signals and it was unclear where this noise was coming from. Therefore, some members of the software team came to assist which slowed down the software production. Additionally, issues with the E-Ink display delayed Mclaine for a while meaning that there was some time lost for testing. All these losses were overall negligible and did not impede the completion of this project. Furthermore, the software

team was able to do much of their testing independently of the hardware team meaning that once the hardware was completed the software was already ready to be implemented (with minor modifications).

V Design Methodology, Analysis, and Specifications

Design methodology

Due the compressed nature of this development cycles the group chose to adopt the SPRINT design methodology. This method has six main sections as seen in Figure 3 below.

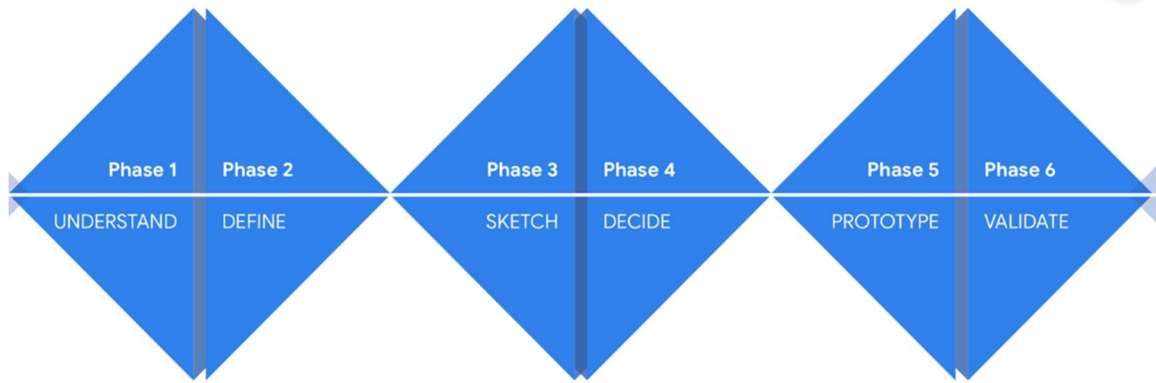


Fig. 3. SPRINT methodology general outline [8]

The first step was to understand and define the problem. As mentioned in the introduction as the world shifts to more green technology solar power is becoming more popular. However, the problem lies in the fact that generally solar panels are very inefficient (about 15 to 20 percent efficient). To solve this problem the maximum power point tracking (MPPT) algorithm was developed. Our goal was to create a cost effective and easily modifiable, cheap, and open-source design that will allow customers to augment the design to their given needs.

Next, the group conducted a literature review to not only determine what solutions there already were to this problem but also to determine alternative design choices we can make. Refer to section III to see the decisions and design alternatives made. Upon project conception we had planned on using an RTOS based system, however based on feedback from our technical supervisor we decided this would not have been a beneficial inclusion and would have taken unnecessary time and resources to implement. Additionally, before we began prototyping the group conducted some simulations of the buck-boost circuit as well as a temporary MPPT algorithm to see what the potential outputs are from the device and components such as the inductors and capacitors. Simulations were also able to assist the group in determining component ratings. MATLAB and SIMULINK were used to complete these simulations, and the topology used for testing looks as follows:

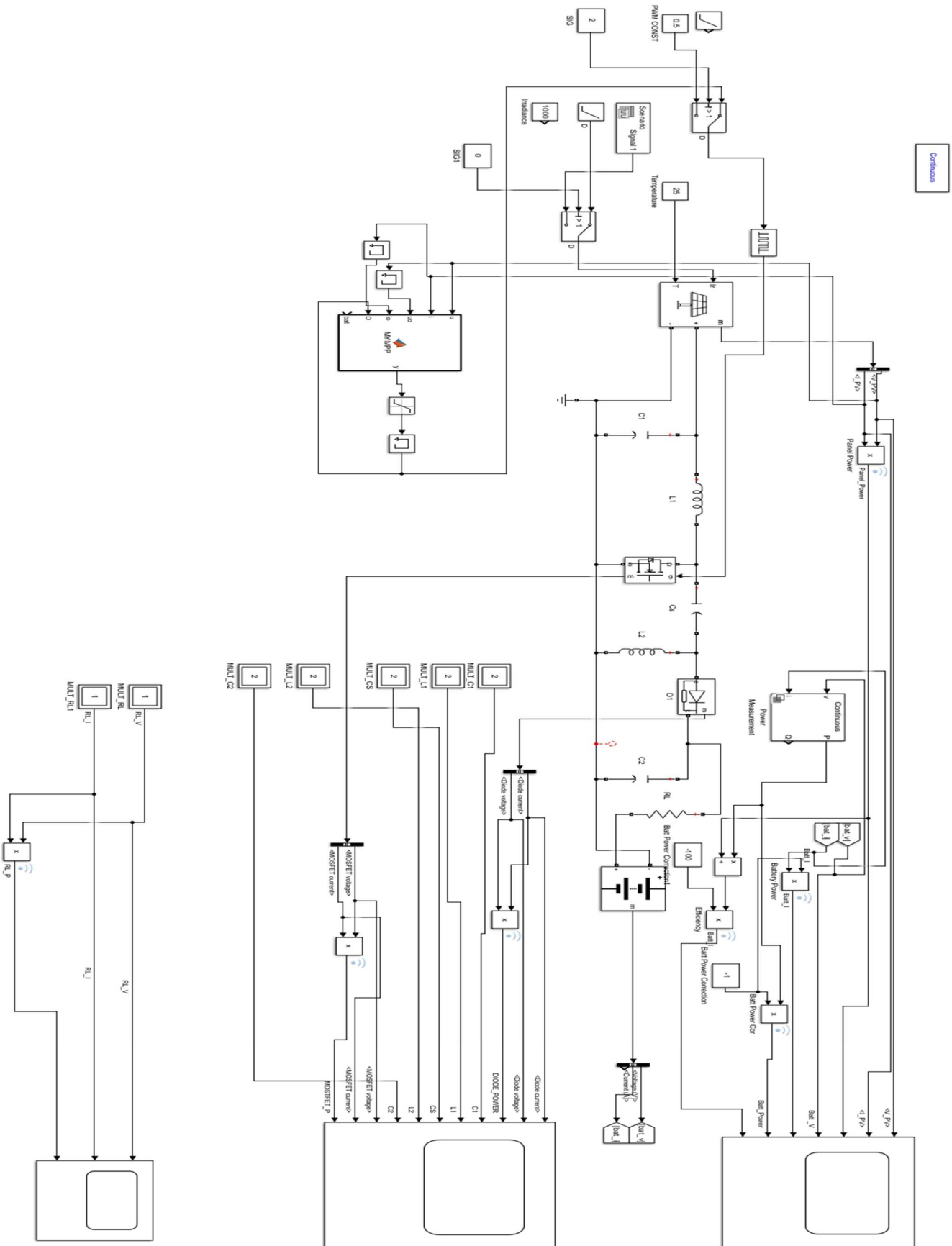


Fig. 4. MLAB simulation topology

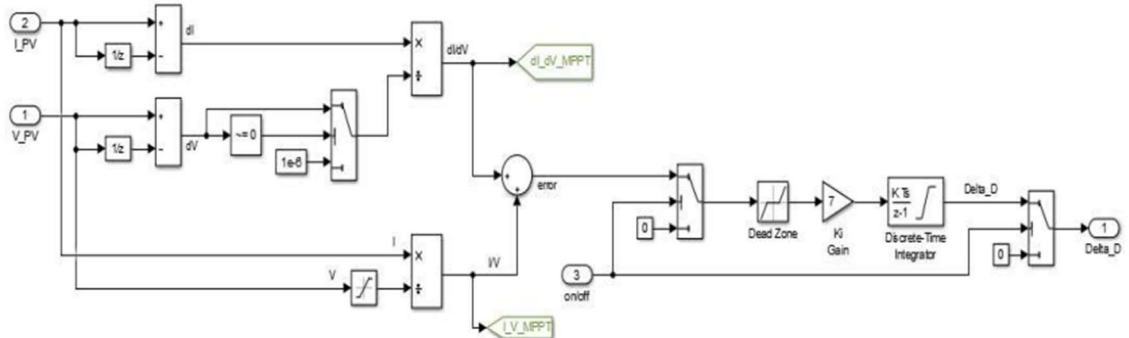


Fig. 5. MLAB simulation of Incremental Conductance MPPT Algorithm [11]

One major limitation of this simulation is its inability to account for partial shading on the solar panel. Partial shading occurs when some cells on the panel are obscured, which drastically reduces current due to the series connection of the cells. Since the output power from the panel is limited by the lowest-performing cell, even a small amount of shading can significantly impact overall efficiency. While this phenomenon was observed during testing, it could not be replicated in the simulation, which assumes full solar panel power (100W in our case) and that all cells are fully illuminated. In practice, however, partial shading can have a substantial effect, especially in panels with cells connected in series. This issue will be further explored in the testing section of this report. Additionally, due to time constraints, we only tested the incremental conductance MPPT algorithm and did not evaluate other MPPT algorithms.

Firstly, this simulation is designed using a single-ended primary inductor converter (SEPIC) which is a type of buck-boost converter. During the literature review we had identified that we would like to use a buck-boost converter, however upon further inspection there are various types of buck-boost topologies. The traditional buck-boost and the flyback topologies (as seen in the Figure X and Y circuits) could work however would require additional components which can lead to increase costs. A buck-boost converter outputs an inverted signal which mean that if this topology were used and additional rectifier would be required and tuned to correct the output. As for the Flyback converter the presence of a transformer in the circuit creates many complications in terms of noise injected into the output as well as will take up more area compared to that of either the buck-boost or the SEPIC. When the simulation was done using buck-boost and flyback it was found that in general there was more noise on the system and an increased chance for higher losses (either from the transformer or the added rectifier). Another benefit of the SEPIC converter is that it is capable of handling a larger range of input voltages. This is a major advantage as polar panels do not provide a reliable input voltage as they are highly dependent on the external environmental conditions.

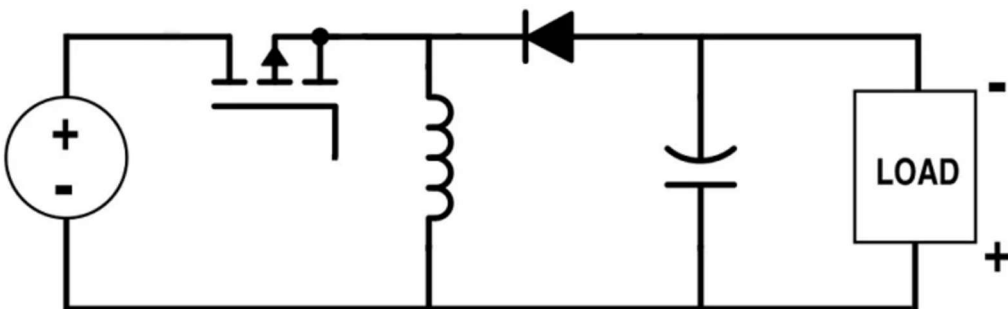


Fig. 6. Buck-Boost Circuit

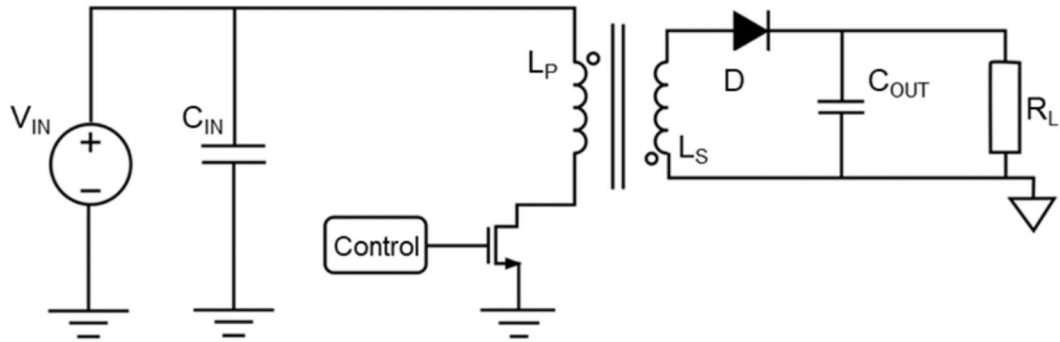


Fig. 7. Flyback Converter

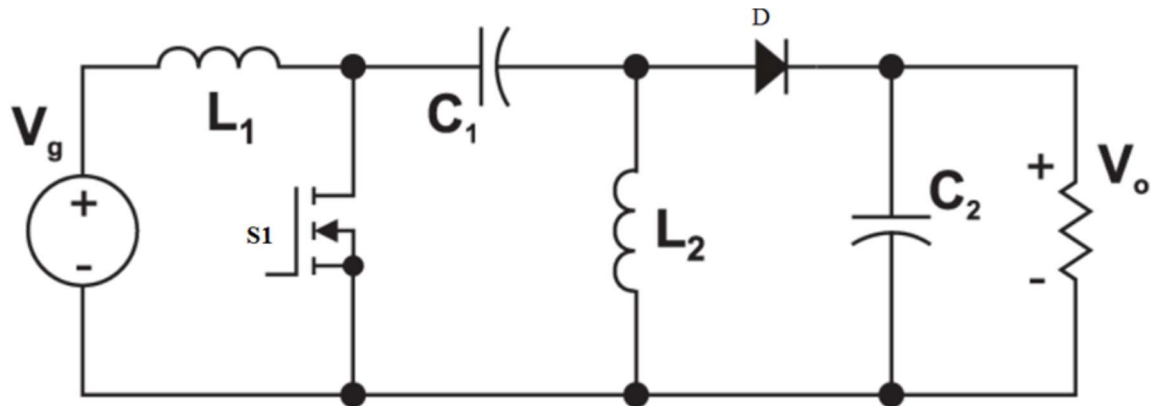


Fig. 8. SEPIC Converter

Another effect that was not considered until after the simulations was the difference between a continuous and discontinuous operation. If the L1 inductor is sized too small it is possible that while on the discharge cycle the inductor may discharge too quickly, cause a brief period of no current flowing. Whereas continuous mode allows the inductor to be in a state of either charging or discharging. Discontinuous operation is not commonly used as it causes lots of large transients as the circuit acts as though it is starting up every cycle causing the current and voltage to spike every charging cycle. These transients can cause damage to the other peripheral components thus reducing the overall longevity. The discontinuous mode however does increase efficiency because all the energy stored in the inductors is being consumed, and switching losses are also reduced. We sized the inductors based on operating in the continuous mode as the power draw for the selected solar panel was 100W and typically discontinuous mode is used for circuits with power draws of less than 50W. To simulate these conditions, we can modify the irradiance level of the panel.

On the rising edge of the voltage waveform the inductor begins to charge and store current and then on the falling edge when the voltage drops to a negative polarity the inductor is discharging. Looking at Figure X, it can be seen that the current finishes discharging before the end of the cycle and before the inductor can change polarity back into the charging region thus leading to the voltage and current being stuck as 0V for a short duration. If the inductor value gets too low that plateau will get larger and if it gets too large then the risk of component damage increases as well as the chance of a brown out across the board. Figure Y depicts the continuous mode operation where there is a smooth sawtooth and square wave curve for the current and voltage respectively.

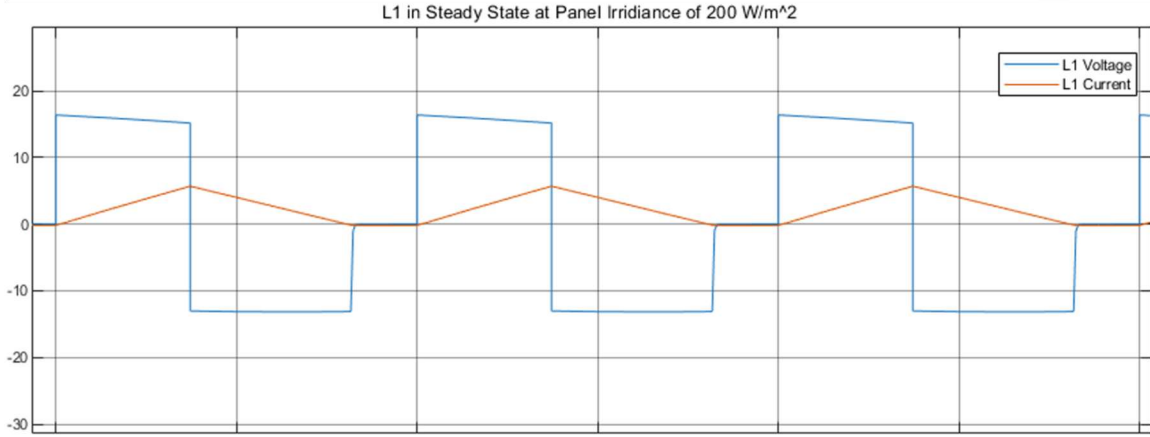


Fig. 9. Discontinuous mode at 200 W/m²

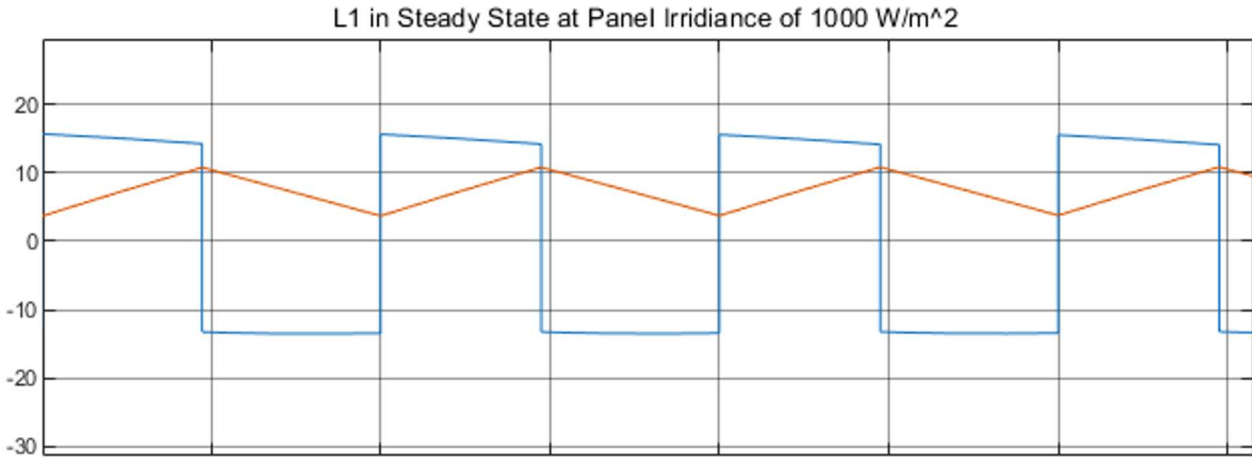


Fig. 10. Continuous mode at 1000 W/m²

We then ran a Irradiance sweep to check the output of the panel and get an idea of what the PWM should be as the irradiance of the panel increases. As the irradiance level increases the panel current and therefore the power increases as the intensity of the light on the panel increases. Additionally, the PWM increase to a limit of about 50%. These conditions were used as a reference during testing. The output results from the simulation can be seen below. There were other graphical outputs done using the simulation however many of them were not deemed relevant for this report but can be found in the Appendix.

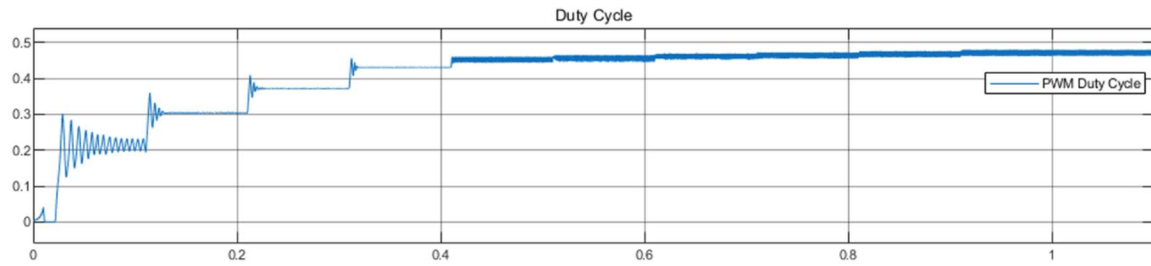


Fig. 11. Change of duty cycle as Irradiance increases

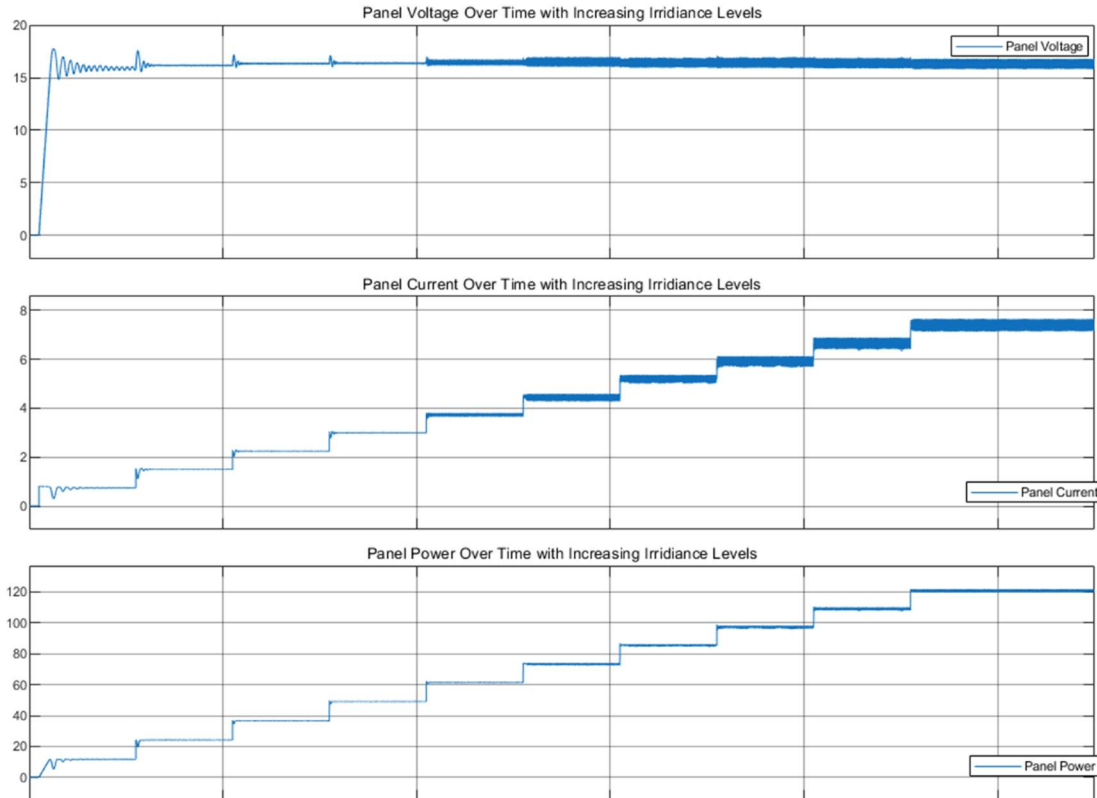


Fig. 12. Solar Panel Voltage, Current, and Power as Irradiance level increases

Specifications

Before we began prototyping, we used the simulation to help determine the component values and design specifications that can be used from component selection during prototyping. To carry out the calculations for preliminary values, maximum and minimum values for input and output current and voltage must be determined. Based on the solar panel rating of 100W maximum. The following table shows the expected maximum input voltage from the panel, as well as the desired output from the battery to the load:

$V_{In(min)}$	5 V
$V_{In(max)}$	50 V
V_{Out}	15 V
I_{Out}	8 A
PWM Frequency	50 kHz
Diode Voltage	0.7 V
Temp Range	15 to 100 deg C

The PWM is based on the maximum output frequency from the STM32 microcontroller. Furthermore, using these specification values the components were calculated using the following formulas:

Duty Cycle

**Assuming Diode Drop of 0.7 V

$$D_{max} = \frac{V_{out} + V_D}{V_{in(min)} + V_{out} + V_D} = \frac{15 + 0.7}{1 + 15 + 0.7} = 0.9401$$

$$D_{min} = \frac{V_{out} + V_D}{V_{in(max)} + V_{out} + V_D} = \frac{15 + 0.7}{50 + 15 + 0.7} = 0.239$$

Inductor

$$\Delta I_L = I_{out} \times \frac{V_{out}}{V_{in(min)}} \times 20\% = 8 A \times \frac{15}{1} \times 20\% = 24 A$$

$$L_1 = L_2 = \frac{V_{in(min)}}{\Delta I_L f_{SW}} D_{max} = \frac{1 V}{24 A \times 50 KHz} \times 0.9401 = 0.783 \mu H$$

Coupling Capacitor

$$I_{CCP(rms)} = I_{out} \times \sqrt{\frac{V_{out} + V_D}{V_{in(min)}}} = 8 A \times \sqrt{\frac{15 + 0.7}{1}} = 31.699 A$$

For 5% Ripple, Minimum Capacitance:

$$C_{CCP} \geq \frac{I_{out} D_{max}}{5\% \times V_{in(min)} f_{SW}} = \frac{8 A \times 0.9401}{5\% \times 1 V \times 50 KHz} = 3.008 mF$$

When starting the design process, we initially selected preliminary values for components that were deliberately scaled up to account for potential larger transients, especially during startup. This was done to ensure that all components in the system could withstand significant current or voltage spikes that might occur. By incorporating this safety margin, we aimed to protect the components from stress and potential damage due to sudden surges or fluctuations in power. This approach not only enhances the overall reliability of the system but also helps to prevent failures and ensure stable operation under varying conditions. By anticipating and accommodating these potential transients, we can better safeguard the integrity and longevity of the design.

VI Design Prototype, and Testing

Design Prototype

Software Design

To begin the software, design an outline of the state flow was created. This allowed us to have a good understanding of how the device moves from one condition to the next and assisted us in knowing what measurements to take to make these state changes. In this regard a UML state diagram was made as shown in Figure 13. Additionally, since the PWM signal is running at 50kHz corresponding to a 20us period we chose a sampling rate of 3 times the PWM period (meaning 60us and 16.67GHz). This ensures we take sufficient samples to represent the measurement waveforms.

On start the test solar function gets the current and voltage from the panel and battery to check that there is some input for the device to start. If the battery voltage is 12.5V the VBAT_OK flag is set and the load is powered on. 12.5V is the minimum safe voltage that can safely power the load without causing damage to the battery.

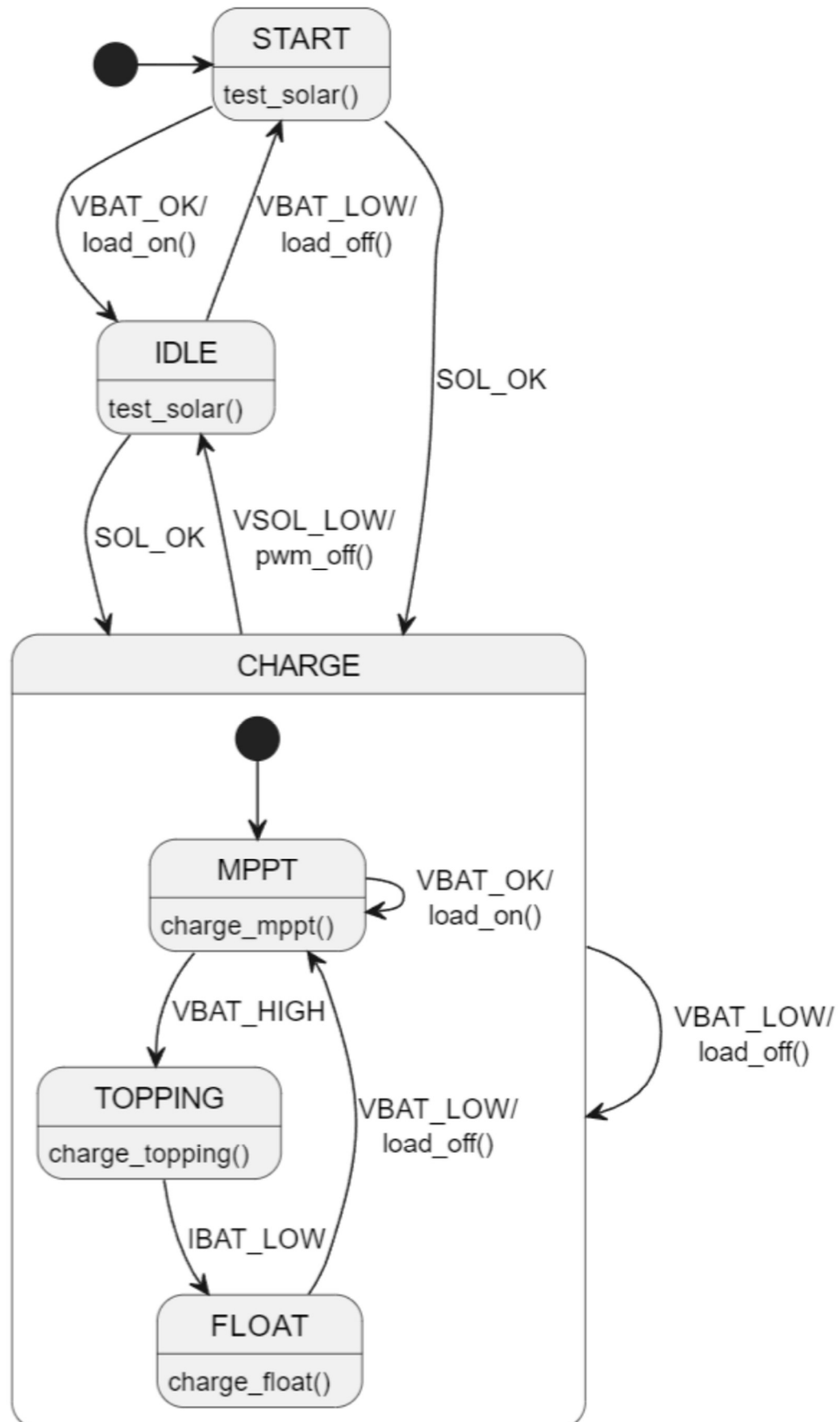


Fig. 13. UML State Diagram

Alternatively, if the battery voltage is 11.75V which is the minimum voltage for the battery to be still healthy. If this voltage drops below 11.75V the battery may be damaged and therefore instead of powering on the load the VBAT_LOW flag is set and the device does not turn on the load to preserve the battery. The difference between VBAT_OK (12.5V) and VBAT_LOW (11.75V) is a buffer that allows for a voltage drop when initially loading the device. Without this buffer, when the load powers on the voltage may drop below the 11.75V threshold and the device will turn off the load as the state then sets the VBAT_LOW flag. The final condition from the start block is the SOL_OK flag. This checks the current and voltage from the panel. The test_solar() function briefly turns on the PWM at 30% (this is an arbitrary value we chose for sampling) to sample the short circuit panel conditions to check if there is a current from the panel before moving into the charge state.

Next the state machine moves into the charge block where the MPPT algorithm is implemented. The incremental conductance algorithm adjusts the PWM to the MOSFET's which effectively change the loading seen by the solar panel in order to track the optimal power point. The MPPT block also checks to make sure the battery voltage is okay and will power on the load (unless it's already on) once the battery has been charged to a sufficient level. The algorithm will stay in the MPPT block until the battery voltage charges up to 14.7V (the maximum safe charging limit of a lead acid battery) and the VBAT_HIGH flag is set. This is typically called the bulk-charging phase. In the topping mode the voltage is held at 14.2V until the battery current drops to 0.65A. The purpose of topping mode is to saturate the battery to balance out the voltage in each cell. As the battery saturates the current drops which is the condition that is checked for to move to the float stage. Float mode is used as more of a trickle charge to maintain the battery voltage at a healthy 13.5V. In float mode there is a 100mA to 400mA trickle charge flowing into the battery. While in float mode if the VBAT_LOW flag is set this means that the load is discharging the battery faster than it can be charged. Therefore, the load is switched off and the state returns to charging mode to get the battery voltage back up. Lastly, if the solar panel voltage drops to a level that the device is unable to charge to battery the device exits charging mode and returns to the idle state until the solar power is restored. Figure 14 is a image of the state table used to move throughout the state diagram:

Current State	Next State	action	V Sol		V Bat		I Bat		EVENT
			OK	Low	High	OK	Low	High	
START/HALT	START	Nothing		x			x	/	VBAT_LOW_VSOL_LOW
	IDLE	load_on		x	x	x		/	VBAT_OK_VSOL_LOW
	MPPT	Charge_mppt	x			x	x	/	VBAT_OK_VSOL_OK
	FLOAT	Charge_float	x		x			/	VBAT_HIGH_VSOL_OK
IDLE	IDLE	Nothing		x	x	x		/	VBAT_OK_VSOL_LOW
	START	Halt		x			x	/	VBAT_LOW_VSOL_LOW
	MPPT	Charge_mppt	x			x	x	/	VBAT_OK_VSOL_OK
	FLOAT	Charge_float	x		x			/	VBAT_HIGH_VSOL_OK
MPPT	MPPT	Charge_mppt	x			x	x	/	VBAT_LOW_VSOL_OK
	START	Halt		x			x	/	VBAT_LOW_VSOL_LOW
	IDLE	stop_pwm		x		x		/	VBAT_OK_VSOL_OK
	MPPT	load_on	/		x			/	VBAT_OK_VSOL_OK
	START	stop_pwm	/		/			x	IBAT_HIGH
	TOPPING	Charge_Topping	x		x			/	VBAT_HIGH_VSOL_OK
	TOPPING	Charge_Topping	x		x			/	VBAT_HIGH_VSOL_OK
TOPPING	START	halt		x			x	/	VBAT_LOW_VSOL_LOW
	IDLE	stop_pwm	x	x	x			/	VBAT_OK_VSOL_OK
	FLOAT	Charge_float	/		/			x	IBAT_LOW
	FLOAT	Charge_float	x		/			/	VBAT_LOW_VSOL_LOW
FLOAT	START	Halt		x			x	/	VBAT_LOW_VSOL_LOW
	IDLE	stop_pwm	x	x	x			/	VBAT_OK_VSOL_OK
	FLOAT	Charge_float	x		/			/	VBAT_LOW_VSOL_LOW

EVENT LIST	
0	VBAT_LOW_VSOL_LOW
1	VBAT_LOW_VSOL_OK
2	VBAT_OK_VSOL_LOW
3	VBAT_OK_VSOL_OK
4	VBAT_HIGH_VSOL_OK
5	IBAT_HIGH
6	IBAT_LOW
"/	= Don't Care

Fig. 14. State Table

Finally, in order to program the ADC the conversion between real and analog values it must be considered. We created a chart that assists in adjusting the ADC value into real values for displaying and calculation values. Figure 15 shows the scale factor used based on the voltage divider found in the hardware and based on the max and minimum voltage or current values. The calculation for the scale is as follows:

$$Scale = \frac{R1}{(R1 + R2)} = \frac{30}{240} = 0.125$$

Voltage Divider							
Inputs	Min	Max	R1 (K ohms)	R2 (K ohms)	Scale	Out min (v)	Out max (v)
V _{solar}	0	25		30	0.125	0	3.125
V _{bat}	0	15		30	0.222222222	0	3.3
I _{solar}	0	5			0.4	0	2
I _{bat}	0	5			0.2	0	1
I _{load}	0	3			0.1	0	0.3

Next the ADC count per unit voltage we calculated based on the ADC max value and the voltage range:

$$Count \text{ per Volt} = \frac{4096 \text{ Counts}}{3.3V} = 1241$$

These values were used to scale the real voltage and encode it as an analog value that the ADC can use as shown in the chart below:

Process Name	Process Value	units	Scaled Voltage	Scaled Value (C Code)	Actual Value
VSOL_OK	1	V	0.125	155	0.999194198
VBAT_OK	12.5	V	2.777777778	3447	12.4991942
VBAT_LOW	11.75	V	2.611111111	3240	11.74858985
VBAT_HIGH	14.7	V	3.266666667	4054	14.70024174
VOLTAGE_TOPPING	14.2	V	3.155555556	3916	14.19983884
VOLTAGE_FLOAT	12.7	V	2.822222222	3502	12.69863014
IBAT_LOW (C/100)	0.65	A	0.065	81	0.652699436
ISOL_OK	0.1	A	0.04	50	0.100725222

$$Scaled \text{ Voltage} = Voltage * Scale * Count \text{ per volt} = 12.5 * 0.222 * 1241 = 3447$$

To reclaim the voltage, we just do the same operation in reverse solving for the scaled voltage. Additionally, it must be understood that intrinsic to any physical components there will be losses and inaccuracies. This mean that the ADC will have some variation as compared to the real values. To test for these discrepancies, we measured the real input values and compared that to the output displayed on the E-Ink display built into the STM32. Continuing these calculations the offset can be found.

Battery Compensation		
ADC Value	Calculated Real Value	Actual Real Value
3294	11.94439968	12.74
Real Offset	ADC Offset	
0.795600322	987	

Even after all the compensation the data value were slightly off compared to that of the values read by the oscilloscope and multimeters, however they were much closer to the real values than without the offset. Due to limited time, it was not deemed necessary to fully rectify this issue as the prototype serves as more of a proof of concept.

Hardware Design

First was designing the SEPIC converter. The values that were used for the components was calculated previous in the design methodology section. A few modifications had to be made in order to accommodate the voltage and current monitoring as well as be able to handle inputs and outputs from the STM32. The 100uF cap at the input terminals act as a filter to ensure that a proper DC signal is entering the SEPIC converter. 100uF was used because during testing with a smaller cap there was a significant amount of noise on the system thus skewing the data going into the STM causing false state changes or brownouts. Anything larger than 100uF we decided would be too expensive for the purposes of this project. Furthermore, the two voltage dividers were used to scale the voltages into the STM as shown in the software section, the values were dictated by the limitations to the input of the STM, these scaling factors were explored in the software design section so will not be explored further here.

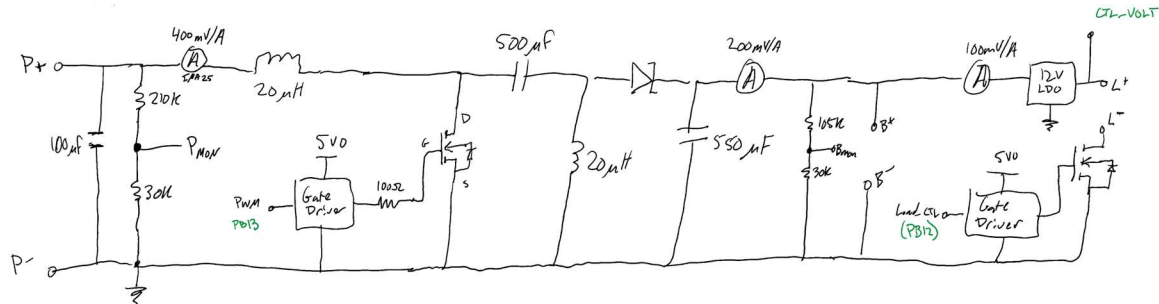


Fig. 15. Overall Circuit Diagram

Another scenario we considered was what would happen if more than one solar panel was used. This would vastly increase the power entering the circuit meaning that the components would need to be scaled up even further. With two panels it was possible to overload the STM ADC causing damage to the controller. One idea we looked into was to use an additional voltage divider for PMON and BMON. Then we can tune each divider to be able to handle higher voltages and one that could handle lower voltages. This would also serve to increase the resolution of the data to the ADC. However, because this prototype was built with only one panel we felt that it was unnecessary to spend more resources pursuing this design any further.

When purchasing components the most cost-effective solution was to use development boards a triple pack of current sensors with different current ratings. Therefore, we decided to place the current sensor with the highest resolution on the first branch that measures the solar panel current. The next two current sensors measure the battery current and the load current respectively. Regardless of the difference in resolution the maximum current that the sensors can handle is 15A maximum. There are two configurations for these sensors, unidirectional and bidirectional configuration. Our design uses the unidirectional mode. We chose this because we are dealing with direct current and it should always flow in one direction which is the mode that unidirectional mode is for. To calculate the current, we use the following equation:

$$\frac{Voltage(mV)}{resolution(\frac{mV}{A})} = amperage$$

Each current sensors layouts were identical and depicted in Figure 16. It can be seen that each of the sensors have an operational amplifier configured as a voltage follower. These op-amps act as an input buffer to isolate the external circuitry from the STM and avoids excessive loading on the STM. The STM can only be loaded with 50kOhm max and without these buffers there was a large amount of interference on the input pins leading to reading that was about half of the expected value. Similarly these buffers were also included on the input to the STM coming from both PMON and BMON.

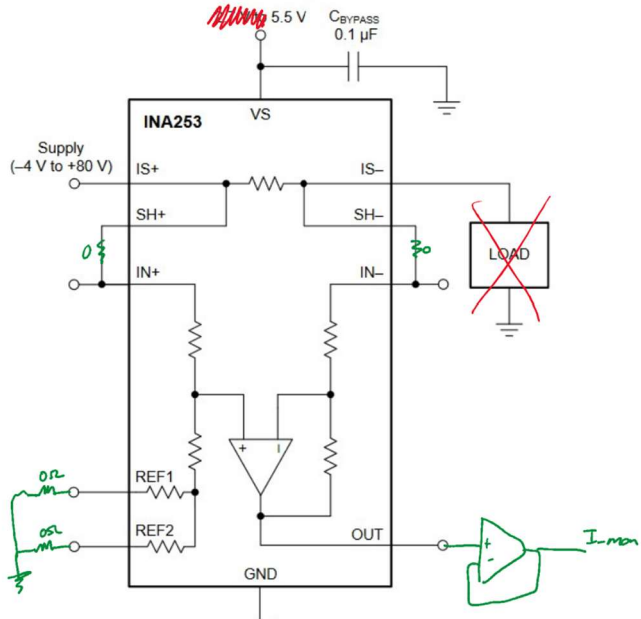


Fig. 16. Current Sensor Layout with Added Peripherals

The STM outputs to the two gate drivers. The first driver controls the FET for the SEPIC converter. One problem we continued to run into was the PWM signal was noisy and there was a significant amount of ringing (this can be seen in the waveforms in the testing section) which caused the FET to turn on unexpectedly. By adding a resistor to the gate of the FET the ringing was reduced and we no longer experienced unexpected switches. Additionally, as the power from the solar panel increased the duty cycle of the PWM increases but this also leads to the FET switching more frequently. This caused the FET's to get very hot thus we had to include heat sinks in order to reduce the heat to increase the longevity of the FET's. Continuing on, The second gate driver allows the STM to connect and disconnect the load based on the state flow. The input to this driver is completely DC and therefore is not impacted by the same ringing as the first FET and therefore the resistor was not needed. Next, on the output there was a voltage rectifier (LDO) that rectified the battery voltage to a more consistent 12V DC. However, it also servers to current limit the load to 3A. This value can be increased or decreased by modifying the LDO ratings to get more current on the output.

Finally, the CTL_Volt rail connects to an additional buck-boost regulator that will rectify the input voltage down to 5V. This was included as we had originally hoped to power the STM and gate drivers off of this rail after the device had started up. One issue we had was because this circuitry was located at the load when the load was disconnected the whole board would power down which was a major limitation. Unfortunately, due to time limitations the capability the device to power itself was not a feature that we had time to flush out and test so therefore we left it out of this first prototype.

TPS63070 Buck-Boost Regulator

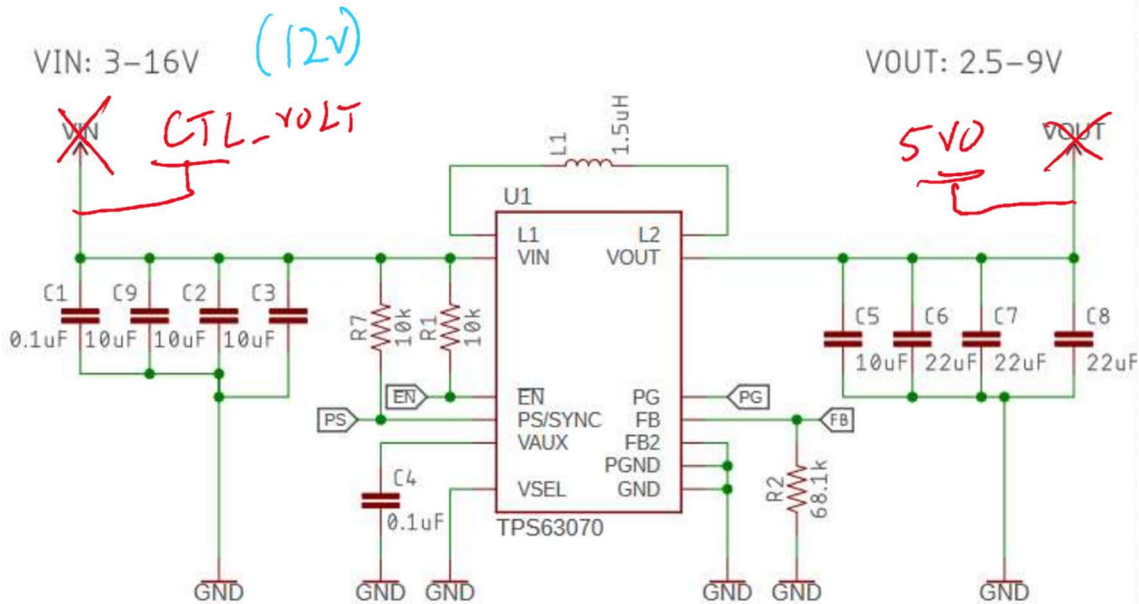


Fig. 17. Expected Charging Cycle

As for an enclosure, we 3D printed a simple case for the device. We did not have time to design a fully weatherproof enclosure and for the purposes of presenting the device to the public we wanted to keep the top exposed. The final overall prototype looked as follows.

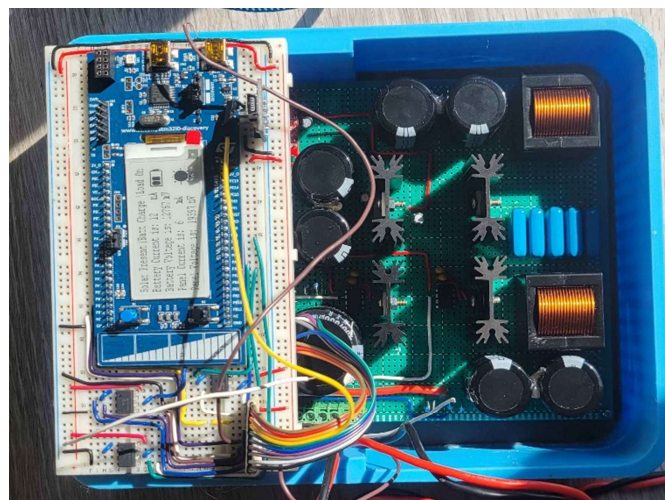


Fig. 18. Overall Prototype

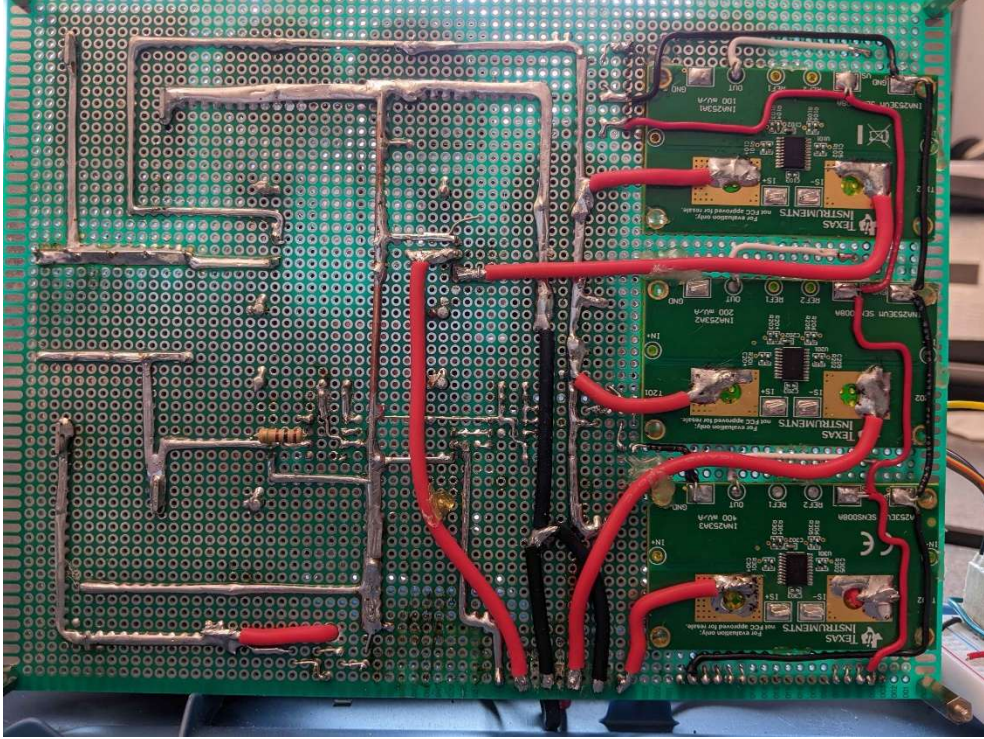


Fig. 19. Underside of Prototype Housing the Current Sensors

VII Prototype Testing

Before we began testing, we created a basic test plan to guide our evaluation process. This plan was intentionally kept simple due to the complexity of our project and the limited time available. To maximize efficiency, we decided to conduct all our testing after the completion of both hardware and software development. This approach was chosen to consolidate testing efforts and streamline the evaluation phase. It's important to note that this strategy did not include modular testing during the development process. Modular testing, which involves evaluating individual components or segments of the system separately, was not performed. This step is crucial for verifying the functionality of specific code sections and hardware components throughout development. Instead, we focused on a comprehensive testing phase at the end to assess the integrated system as a whole. For detailed information on the testing procedures and criteria used, please refer to the test plan provided in the appendix section of this report. This document outlines the specific tests performed and serves as a reference for understanding our testing approach and methodology.

Test setup

The test setup we used began with connecting the solar panel to the input terminals of the MPPT (Maximum Power Point Tracker) charger. This connection allows the solar panel's generated energy to be processed by the MPPT charger. Next, connect the output terminals of the MPPT charger to the battery. This step ensures that the energy optimized by the MPPT charger is directed into the battery for storage. It is crucial to double-check that all connections are secure and correctly made to prevent any issues with the system's operation. For accurate measurement and monitoring, set up the measurement equipment. Connect a multimeter in parallel with the battery terminals to measure the voltage across the battery. This will provide real-time information about the battery's charge level.

Additionally, use a clamp meter to measure the current flowing through the system. Place the clamp meter around either the positive or negative wire to capture current readings. If you have a data logger available, set it up to record real-time data on both voltage and current. This will allow you to monitor the system's performance continuously and make informed adjustments as needed.

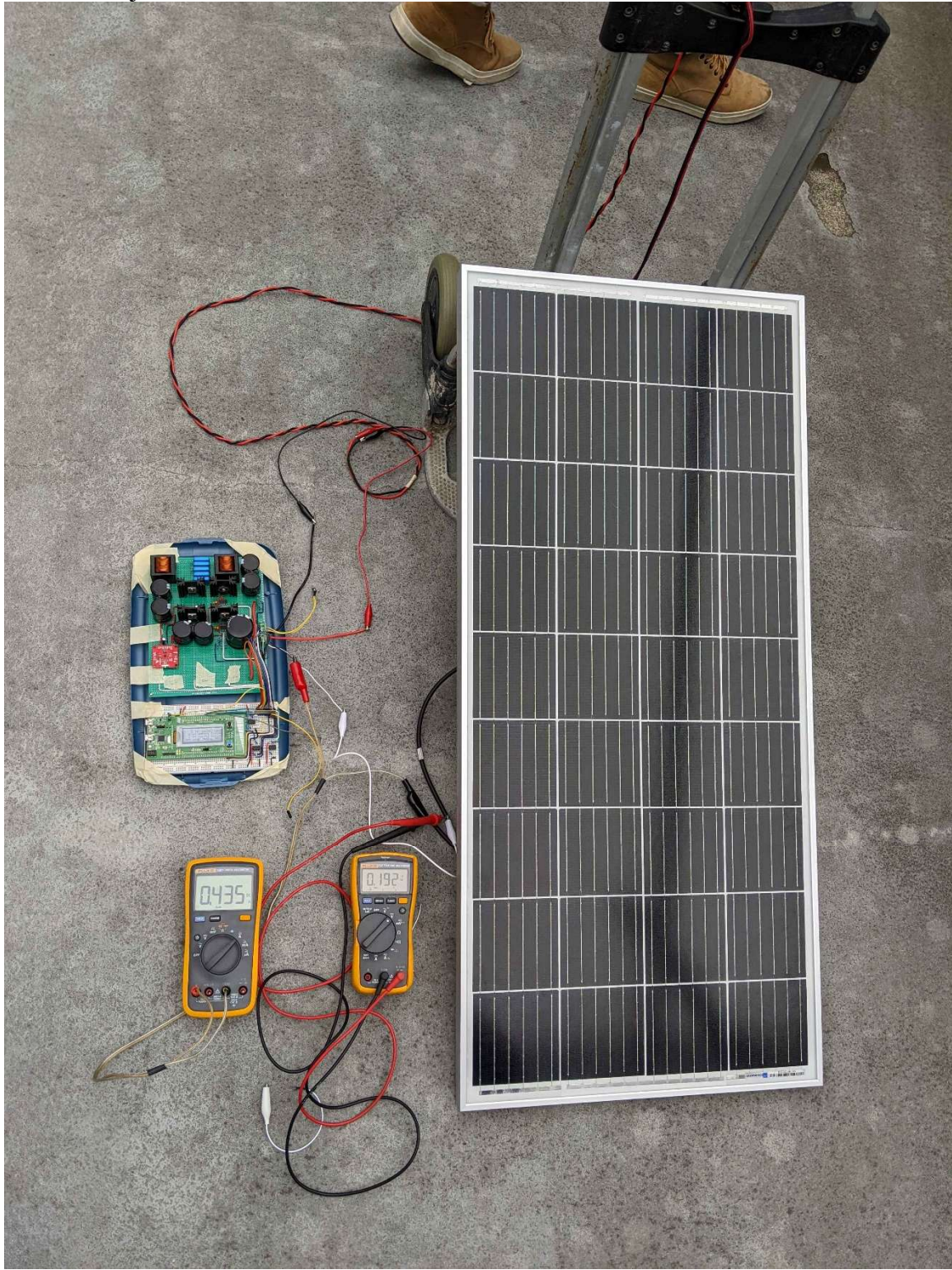


Fig. 20. Overall Testing Setup without Clamp Meters

Initial Startup and Debugging Tests

Full-sunlight test

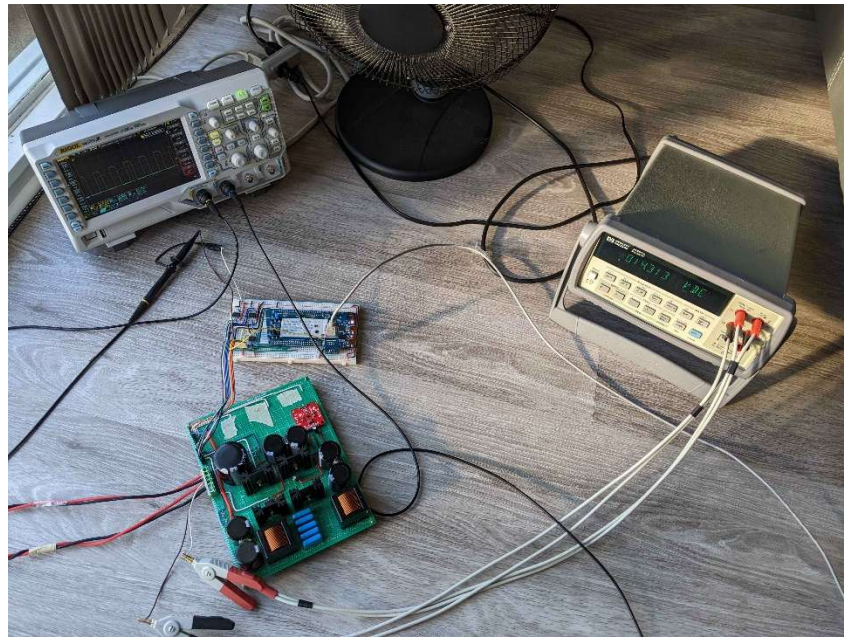


Fig. 21. Full-Sunlight Test Setup

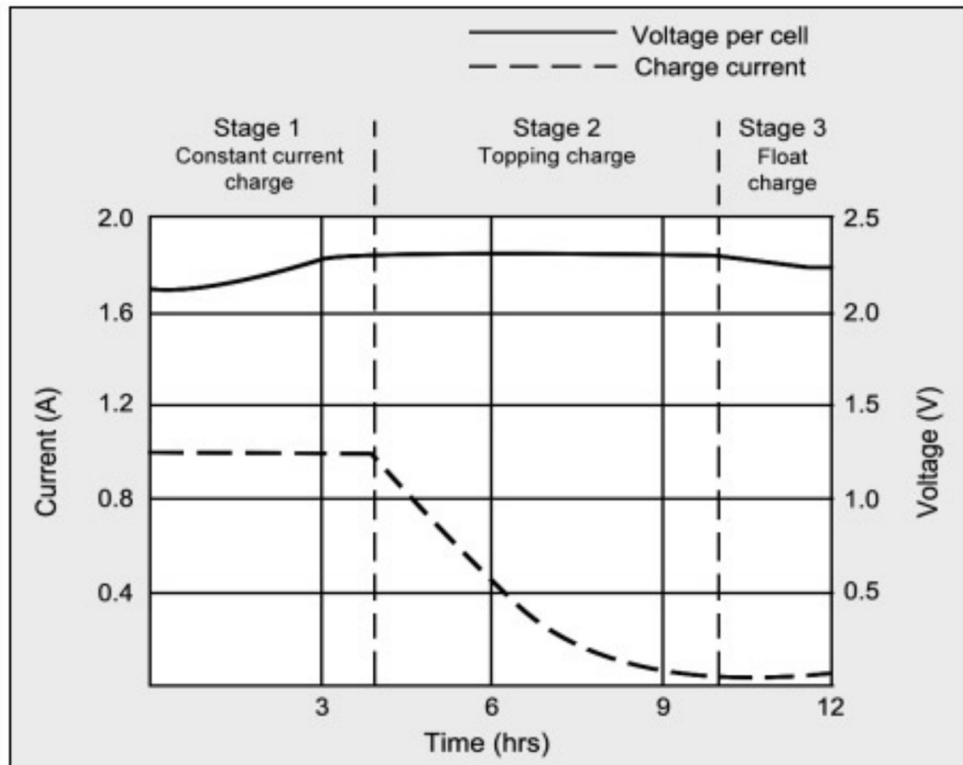


Fig. 15. Expected Charging Cyle

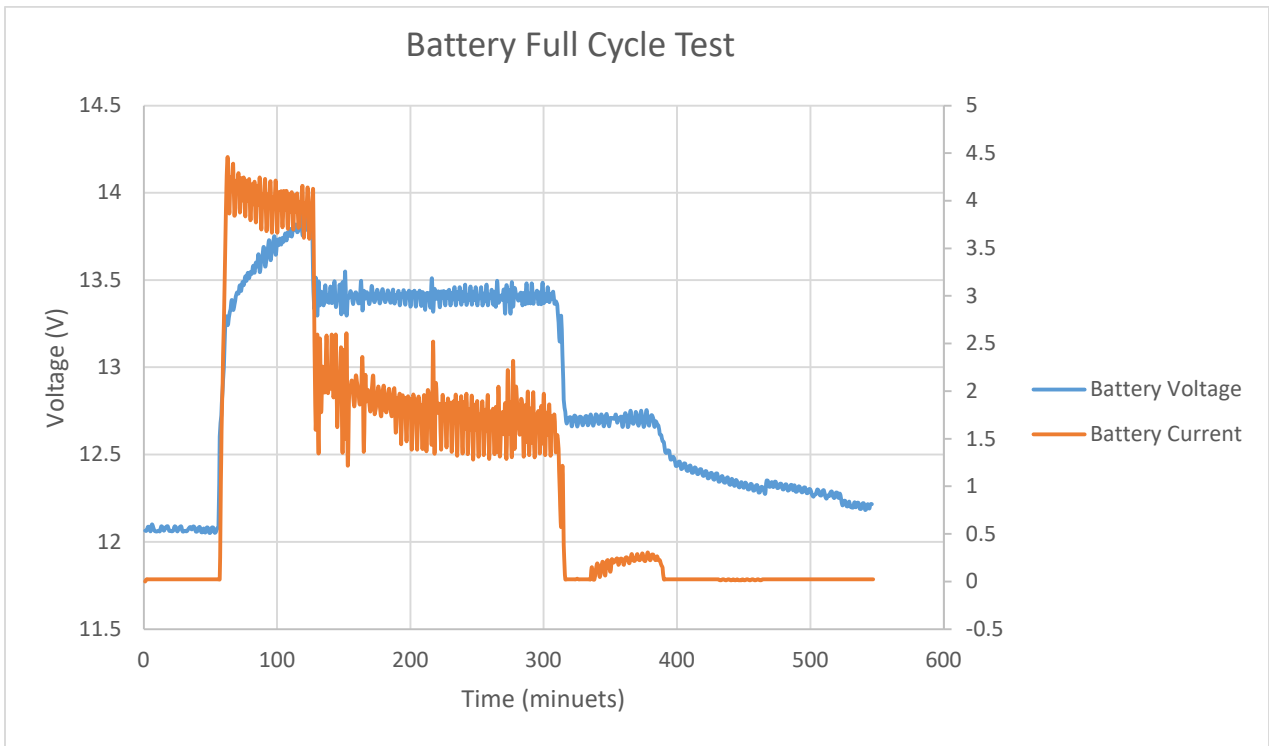


Fig. 15. Full Cycle Testing

Efficiency Test

Discarded tests

Due to time constraints and the lack of baseline data, we were unable to perform several important tests for our MPPT system. We did not conduct load testing to see how the system handles different power levels, nor did we test for over-current and over-voltage to ensure it can handle electrical issues safely. We also missed out on testing how the system performs under partial shading, which affects efficiency when the solar panel is not evenly lit. Long-term testing, which would provide insights into the system's durability over time, was also not possible. Given these limitations, we focused on essential simulations and core functionality testing. In future phases of development, we plan to address these missing tests to fully ensure the system's reliability and performance under various conditions.

VIII Cost Analysis

Direct Costs

For the direct costs we kept track of all purchases utilizing a Bill of Materials (BOM). These only listed the components that were purchased including extra for testing and prototyping purposes.

- Products and Materials:** Costs for purchasing components such as solar panels, buck-boost converters, batteries, and other hardware:

Part	Description	Unit Price	Number U	Price
LM2904N/NOPB		\$1.88	5	\$9.40
513102B02500G	HEATSINK TO-220 W/PINS 1.5" TALL	2.19	4	\$8.76
IPA045N10N3GXKSA1	MOSFET N-CH 100V 64A TO220-FP	\$4.10	1	\$4.10
IRFB7545PBF	N-Channel 60 V 95A (Tc) 125W (Tc) Through Hole	\$1.40	1	\$1.40
INA253EVM	INA253 1 - Single Channels per IC Current Sense	\$91.53	1	\$91.53
IXDD604PI	Low-Side Gate Driver IC Non-Inverting 8-DIP	\$3.28	3	\$9.84
DSA301150PA	DIODE SCHOTTKY 150V 30A TO220AC	\$2.92	1	\$2.92
B43541B8476M080	CAP ALUM 47UF 20% 600V SNAP TH	7.77	6	\$46.62
1935776	TERM BLK 2POS SIDE ENTRY 5MM PCB	\$0.66	1	\$0.66
KTD500B107M90A0B00	CAP CER 100UF 50V X7R RADIAL	\$32.98	5	\$164.90
CPEX3231H-200MC	FIXED IND 20UH 30A 3.73MOHM TH	\$34.62	2	\$69.24
YR1B10KCC	RES 10K OHM 0.1% 1/4W AXIAL	\$0.88	6	\$5.28
YR1B210KCC	RES 210K OHM 0.1% 1/4W AXIAL	\$0.92	2	\$1.84
	15 X 20CM Protoboard	\$17.59	1	\$17.59
	SparkFun Buck-Boost Converter	\$10.95	1	\$10.95
STM32L0538-DISCO	DISCOVERY STM32L053C8 EVAL BRD	\$36.31	1	\$36.31
ECO-WORTHY 100W Solar Panel 12V		\$109.99	1	\$109.99
65Ah Battery		\$209.99	1	\$209.99
			Total	\$801.32

Fig. 1. A sample graph with labels along x, and y axes. The image has multiple signals represented using different types of lines and identified using a text.

- **Travel Expenses:** Driving to and from the campus to do team meetings and testing, this value is accounting for all members of the team:
 - Travel Costs: \$150
- **Food and Accommodation:** Specifically for food during any late nights on campus working:
 - Meals: \$150
- **Software and Tools:** All the software used and other development tools such as soldering irons and 3D printers were also provided by the University of Victoria:
 - Software Licenses: \$0
 - Development Tools: \$0

Total Direct Costs: $\$801.32 + \$150 + \$150 = \$1,101.32$

Indirect Costs

Assuming a pay structure like an average co-op program throughout the degree the average hourly wage is about \$22/hr and all members worked for about 8 hours per week throughout the semester. Furthermore, assuming all members were paid the same amount the total labor costs are:

- **Labor Costs:** Calculated based on hours worked by the team members.
 - Engineers (100 hours @ \$22/hour): $\$22 * 100 * 5 \text{ members} = \$11,000$

Total Indirect Costs: \$11,000

Funding

- **Sponsorships:** Contributions from the class reimbursements were:
 - Reimbursements: $\$150 + \$250 * 5 \text{ members} = \$1,400$

- Reimbursements were only given for the items that were purchased and therefore is a maximum of \$1,400.

Total Funding: \$1,400

Tentative Pricing and Return on Investment (ROI)

- **Prototype Cost:** The total cost to design and develop the prototype with and without a pay structure:
 - Total Prototype Cost without pay (Direct + Indirect Costs): \$1,101.32
 - Total Prototype Cost with pay (Direct + Indirect Costs): \$12,101.32
 - Total Prototype Cost with funding (Direct + Indirect Costs): \$0
- **Pricing Strategy:** The average price on the market for an MPPT Solar Tracker ranges from \$100 to \$1,500 depending on features that are offered and desired ratings of the unit themselves. 12V rated systems such as our own are closer to the \$150-\$300 range. Meaning to stay competitive to the market our proposed selling point is:
 - Estimated Selling Price: \$175
- **Return on Investment (ROI):** Assuming we make on the low end of sales at only 25 sales per year the projected revenue comes to (this does not consider taxes or company operating costs or anything):
 - Projected Revenue = $\$175 * 25 = \$4,375$
 - $ROI = (\text{Projected Revenue} - \text{Total Prototype Cost}) / \text{Total Prototype Cost}$
 - $ROI = (\$4,375 - \$1,101.32) / \$1,101.32 = 297\%$

Cost Reduction Strategies

- **Bulk Purchasing:** After the development of this prototype, we are much better able to bulk purchase supplies and components needed as we know what we need. Therefore, we can make bulk orders or perhaps curate deals with sellers to get a discount on the component ordering.
- **Alternative Component Selection:** We can further reduce costs by selecting cheaper alternatives for some of the components such as the current sensors or the filter capacitors. Additionally, if this product were to be sold equipment such as a battery and solar panel would not need to be purchased again and can be reused for testing during manufacturing thus saving on cost.

IX Conclusion & Recommendations

There are many avenues for future work and development that could not be implemented due to time constraints. For example, the battery charge controller algorithm is based on Lead-Acid batteries. The charge controller algorithm can be adjusted to allow for the optimal charging of other more complex battery types. A more advanced charge controller algorithm could also allow the PV system to be powered using a smaller battery such as a lithium-ion battery. Furthermore, efficiency can be increased with the development of more sophisticated MPPT algorithms that can better track the maximum power point under rapidly changing conditions. Moreover, exploring algorithms that adapt to varying environmental conditions, including partial shading and temperature variations, to optimize power extraction from the solar panel. MPPT solar chargers can be developed with the assistance of Internet of Things (IoT) to allow users to track their solar efficiencies during long term use operations enabling them to pinpoint which solar panel in an array is not being fully utilized due to panel placement or other

variables. Additionally, further efficiency enhancements to the DC-DC converters to reduce energy losses during the conversion process.

In conclusion, our project addresses the inherent inefficiencies of traditional solar power systems by implementing a Maximum Power Point Tracker (MPPT) algorithm coupled with a buck-boost converter. This innovative approach allows for a broader range of solar panel configurations and minimizes energy losses, optimizing both power output and storage. By enabling a more reliable and efficient utilization of solar energy, our system not only supports continuous operation of devices and extends battery life but also advances sustainable energy practices. This solution aligns with the Engineers and Geoscientists BC (EGBC) Code of Ethics by promoting environmental stewardship and sustainable development. It provides a practical and effective means for maximizing energy efficiency in solar installations, benefiting both residential and commercial users. Our MPPT technology also supports the broader adoption of renewable energy, contributing to reduced fossil fuel dependence and mitigating climate change impacts. Ultimately, our project reflects a commitment to enhancing green energy solutions and demonstrates the practical advantages of integrating advanced technology in renewable energy systems. By harnessing the full potential of solar power, we aim to foster a more sustainable and eco-friendly future.

References

- [1] , S. Paul Ayeng'o, T. Schirmer, K.-P. Kairies, H. Axelsen and D. Uwe Sauer, "Comparison of off-grid power supply systems using lead-acid and lithium-ion batteries," Solar energy, vol. 162, pp. 140-152, 2018.
- [2] , R. Wagner and D. U. Sauer, "Charge strategies for valve-regulated lead/acid batteries in solar power applications," Journal of Power Sources, vol. 95, pp. 141-152, 2001-03.
- [3] , M. Mohanty, S. Prakash and S. Padhee, "Impedance Matching of Photovoltaic System Using DC-DC Converter," in Smart Technologies for Power and Green Energy. Lecture Notes in Networks and Systems, vol 443, Singapore, 2023.
- [4] , M. M. a. S. S. . J. Saharia, "Comparative Study on Buck and Buck-Boost DC-DC Converters for MPP Tracking for Photovoltaic Power Systems," in 2016 Second International Conference on Computational Intelligence & Communication Technology, Ghaziabad, 2016 .
- [5] , M. S. A. K. R. a. T. T. O. K. Islam, "A Comprehensive Comparison Between Boost and Buck-Boost Converters in Solar MPPT With ANN2020," in 2020 Emerging Technology in Computing, Communication and Electronics (ETCCE),, Bangladesh, 2020.
- [6] , G. L. X. C. A. O. Baba, "Classification and Evaluation Review of Maximum Power Point Tracking Methods," Sustainable Futures, vol. 2, 2020.
- [7] , F. T. Richard Barry, "Free RTOS book and reference manual," FreeRTOS, [Online]. Available: https://www.freertos.org/Documentation/RTOS_book.html. [Accessed 23 06 2024].
- [8] , N. Calder, Boatowner's mechanical and electrical manual: How to Maintain, Repair, and Improve Your Boat's Essential Systems, International Marine/Ragged Mountain Press, 1996.

- [9] , R. W. a. D. U. Sauer, "Charge strategies for valve-regulated lead/acid batteries in solar power applications," Journal of power sources, vol. 95, no. 1, pp. 141-152, 2001.
- [10] , "Battery charging - AGM," Rolls Battery Technical Support, [Online]. Available: <https://support.rollsbattery.com/en/support/solutions/articles/4345-agm-charging> . [Accessed 22 06 2024].
- [11] , W. J, "Design of a Maximum Power Point Tracking with Simulation, Analysis and Comparison of Algorithms," Naval Postgraduate School, California, 2012.
- [12] , Y. M. N. H. B. M. A. I. a. A. M. A. K. Ananda-Rao, "Design of MPPT charge controller using zeta converter for battery integrated with solar Photovoltaic (PV) system," Journal of physics. Conference series, vol. 1432, no. 1, p. 12058, 2020.
- [13] , A. Brooks, "Best MPPT Solar Charge Controllers of 2024," Forbes Home, 09 04 2024. [Online]. Available: <https://www.forbes.com/home-improvement/solar/best-mppt-solar-charge-controllers>. [Accessed 23 06 2024].
- [14] , S. J. I. H. S. P. L.G. Chagas, Ionic Liquid-Based Electrolytes for Sodium-Ion Batteries: Tuning Properties to Enhance the Electrochemical Performance of Manganese-Based Layered Oxide Cathode, ACS Applied Materials and Interfaces, 2019.

Appendix

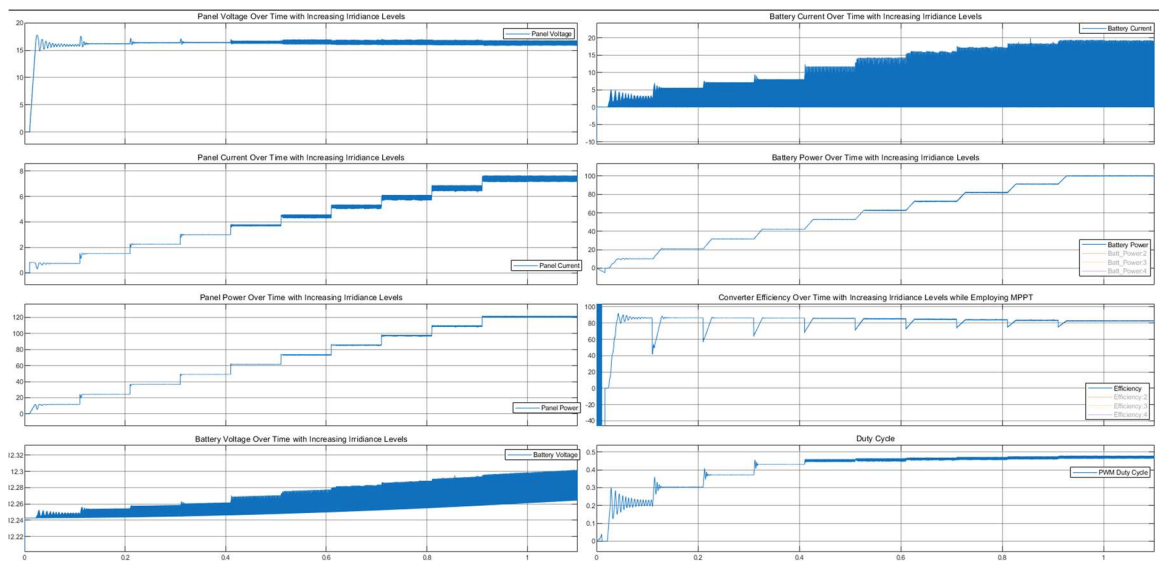
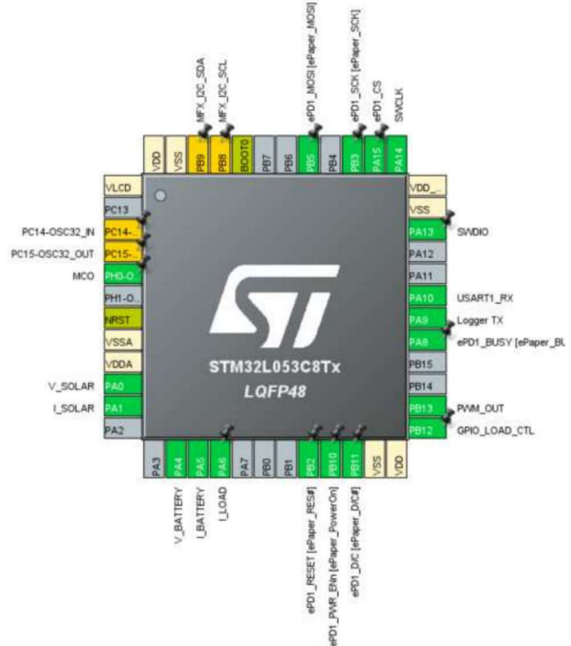
Code of ethics of EGBC

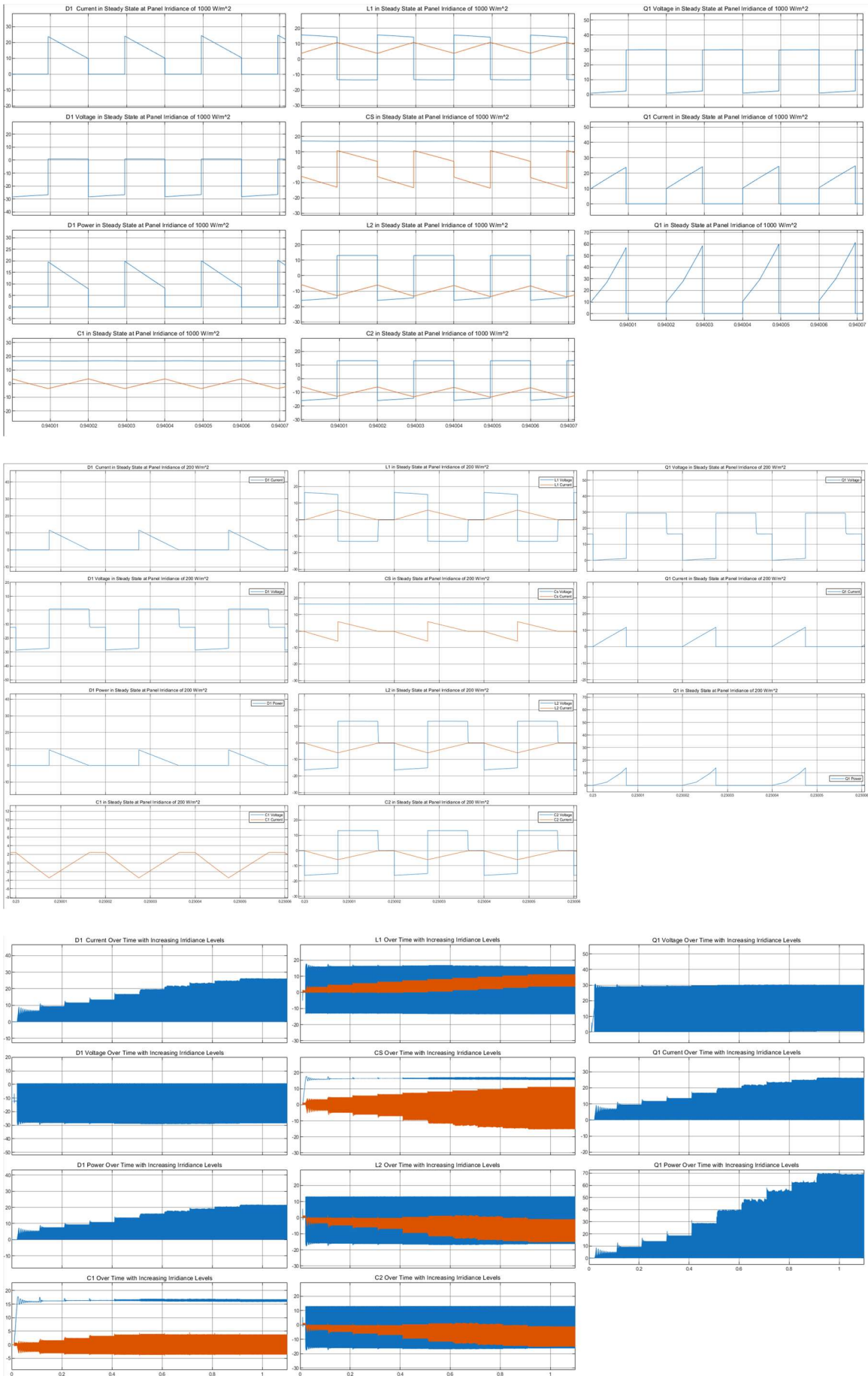
Registrants must act at all times with fairness, courtesy and good faith toward all persons with whom the registrant has professional dealings, and in accordance with the public interest. Registrants must uphold the values of truth, honesty, and trustworthiness and safeguard human life and welfare and the environment. In keeping with these basic tenets, registrants must:

1. Hold paramount the safety, health, and welfare of the public, including the protection of the environment and the promotion of health and safety in the workplace;
2. Practice only in those fields where training and ability make the registrant professionally competent;
3. Have regard for the common law and any applicable enactments, federal enactments, or enactments of another province;
4. Have regard for applicable standards, policies, plans, and practices established by the government or Engineers and Geoscientists BC;
5. Maintain competence in relevant specializations, including advances in the regulated practice and relevant science;
6. Provide accurate information in respect of qualifications and experience;
7. Provide professional opinions that distinguish between facts, assumptions, and opinions;
8. Avoid situations and circumstances in which there is a real or perceived conflict of interest and ensure conflicts of interest, including perceived conflicts of interest, are properly disclosed and necessary measures are taken so a conflict of interest does not bias decisions or recommendations;
9. Report to Engineers and Geoscientists BC and, if applicable, any other appropriate authority, if the registrant, on reasonable and probable grounds, believes that:
 - a. The continued practice of a regulated practice by another registrant or other person, including firms and employers, might pose a risk of significant harm to the environment or to the health or safety of the public or a group of people; or
 - b. A registrant or another individual has made decisions or engaged in practices which may be illegal or unethical;
10. Present clearly to employers and clients the possible consequences if professional decisions or judgments are overruled or disregarded;
11. Clearly identify each registrant who has contributed professional work, including recommendations, reports, statements, or opinions;
12. Undertake work and documentation with due diligence and in accordance with any guidance developed to standardize professional documentation for the applicable profession; and
13. Conduct themselves with fairness, courtesy, and good faith towards clients, colleagues, and others, give credit where it is due and accept, as well as give, honest and fair professional comment.

Website link and the main page image
GITHUB: <https://github.com/bdionello/ECE499.git>
WEBSITE: <https://mpptsolar.my.canva.site/>

Details of data, test results





Test Plan for Solar MPPT Charger

**1. Objective:

- To evaluate the performance and efficiency of the MPPT charger under various conditions and ensure it operates correctly with solar panels and batteries.
-

**2. Equipment Required:

- Solar panel (with known specifications)
 - MPPT charger
 - Battery (for storage)
 - Multimeter (to measure voltage and current)
 - Clamp meter (for current measurement)
 - Load (resistive or electronic)
 - Power supply (for controlled input testing)
 - Oscilloscope
-

**3. Test Setup:

**a. Basic Connectivity:

- Connect the solar panel to the input terminals of the MPPT charger.
- Connect the output terminals of the MPPT charger to the battery.
- Ensure all connections are secure and correct.

**b. Measurement Setup:

- Connect the multimeter in parallel with the battery to measure voltage.
 - Connect the clamp meter around the positive or negative wire to measure current.
 - Set up the data logger if available to record real-time data.
-

**4. Test Cases:

**a. Startup Test:

- **Objective:** Verify correct operation when the system starts.
- **Procedure:** Power the solar panel and observe the MPPT charger's response. Check for correct initialization and charging initiation.
- **Expected Results:** The MPPT charger should start tracking the maximum power point and begin charging the battery without errors.

**b. Full Sunlight Test:

- **Objective:** Assess performance under ideal conditions.
- **Procedure:** Expose the solar panel to full sunlight. Measure the input voltage and current from the panel, and the output voltage and current to the battery.
- **Expected Results:** The MPPT charger should operate efficiently, optimizing power output and charging the battery effectively.

**c. Partial Shading Test:

- **Objective:** Evaluate performance under partial shading conditions.
 - **Procedure:** Apply partial shading to the solar panel (e.g., cover part of the panel with an opaque object). Measure and compare the power output and charging efficiency.
 - **Expected Results:** The MPPT charger should still be able to track and optimize power, though overall output may decrease due to shading.
-

****5. Data Collection:**

- Record input and output voltages and currents for each test case.
 - Note any anomalies or deviations from expected results.
 - Document the performance of the MPPT algorithm in varying conditions.
-

****6. Analysis:**

- Compare recorded data with expected results.
 - Evaluate the efficiency of the MPPT charger and its ability to track the maximum power point.
 - Identify any issues or areas for improvement based on test outcomes.
-

****7. Conclusion:**

- Summarize the performance of the MPPT charger based on test results.
- Provide recommendations for any necessary adjustments or further testing.